ABSTRACT

FERRELL, TIFFANY. Development of an EGFR-targeting Alginate-based Injectable Hydrogel Drug Delivery System for the Improved Treatment of Solid Malignancies. (Under the direction of Yevgeny Brudno).

Systemic distribution of chemotherapeutic drugs results in inefficient drug delivery to the target cancer site, toxic off-target effects, and a narrow therapeutic window. These issues could be remedied by localized drug presentation that does not enter circulation. The development of hydrogel-based drug delivery depots has made progress on this front, with alginate-based hydrogels showing particular promise. Alginate-based hydrogels are biocompatible, chemically versatile, and low in toxicity. When combined with click chemistry, alginate hydrogels have demonstrated increased stability and great potential in producing a drug depot that safely and effectively overcomes the obstacles presented by the systemic distribution of drugs. In this dissertation, a click chemistry-based alginate hydrogel is combined with the chemotherapy drug erlotinib conjugated to a novel sulfone-based linker. This hydrogel system could be injected directly into a tumor or tumor cavity to offer localized, sustained released of erlotinib to susceptible cancers over a prolonged period of time.

Development of an EGFR-targeting Alginate-based Injectable Hydrogel Drug Delivery System for the Improved Treatment of Solid Malignancies

by
Tiffany Ferrell

A thesis submitted to the Graduate Faculty of
North Carolina State University
in partial fulfillment of the
requirements for the degree of
Master of Science

Comparative Biomedical Sciences

Raleigh, North Carolina

2021

APPROVED BY:

_____	_____
Dr. Yevgeny Brudno Chair of Advisory Committee	Dr. Paul Hess
_____	_____
Dr. David Zaharoff	Dr. Duncan Lascelles

BIOGRAPHY

Tiffany Ferrell was born and raised in Concord, North Carolina on November 9, 1995. She completed her undergraduate degree in biology at Pfeiffer University and graduated *summa cum laude.* A life-long interest in animals and medicine drove her to applying to graduate school at North Carolina State University, where she was ultimately accepted into the comparative biomedical sciences PhD program. Through a combination of difficulties associated with a research-based career and a plethora of impactful external factors, Tiffany decided to complete her time in the program with a master's and pursue a teaching-based career path. Today, Tiffany works as a research assistant in Dr. Yevgeny Brudno's lab to complete this master's degree.

ACKNOWLEDGEMENTS

I would like to thank my advisor, Dr. Yevgeny Brudno, for his guidance and support on this project. I have grown substantially as an academic and as a person under his direction.

I would next like to thank my committee for all of their assistance and advice.

I would like to thank all the members of the Brudno Lab for their help, particularly Chris Moody, who has provided me with lots of assistance.

Additionally, I would like to thank Nick Massaro from the Pierce Lab for his help in synthesizing the erlotinib prodrug used in this dissertation.

Finally, I would like to thank my family, friends, and future husband on their much-needed love and support.

TABLE OF CONTENTS

List of Tables……**v**

List of Figures……**vi**

Chapter 1: Introduction……..….**1**

1.1. Current Limitations of Chemotherapy for Solid Tumors……..……..1

1.2. Drug Delivery Strategies…….....…2

1.2.1. Prodrugs……..2

1.2.2. Nanocarriers……4

1.2.3. Drug Depots……7

1.3. Hydrogels as Drug Delivery Systems…….8

1.3.1. Alginate-based Hydrogels……...9

1.3.2. Click Chemistry and Hydrogels……11

1.4. Research Objectives……...13

1.5. References……..16

Chapter 2: Synthesis and Analysis of Erlotinib Prodrug…….30

2.1. Introduction……30

2.2. Methods and Materials……...31

2.2.1. Synthesis of the Erlotinib Prodrug…….32

2.2.2. Compound Preparation and Storage…….....….33

2.2.3. HPLC Analysis……...33

2.2.4. Nanodrop Analysis…….34

2.2.5. Prodrug Kinetics Experiment…….……34

2.3. Results…….35

2.3.1. Synthesis and Structural Confirmation of the Erlotinib Prodrug……35

2.3.2. Baseline Analysis of the Erlotinib Prodrug with HPLC……38

2.3.3. Erlotinib Prodrug Kinetics……..40

2.4. Discussion……42

2.5. References……45

Chapter 3: Synthesis and Analysis of an Alginate Hydrogel containing the Erlotinib-Linker Conjugate…….....48

3.1. Introduction…….….48

3.2. Methods and Materials…….....49

3.2.1. Cell Culture…….….49

3.2.2. Cytotoxicity Experiment…….…….50

3.2.3. Synthesis of t-BCN…….….51

3.2.4. Synthesis of t-BCN Crosslinked Hydrogels……....51

3.2.5. HPLC Analysis……51

3.3. Results…….53

3.3.1. Assessment of Prodrug Cytotoxicity……...53

3.3.2. Synthesis and Purification of t-BCN……...55

3.3.3. Synthesis of Prodrug-Containing Hydrogels……...……56

3.4. Discussion……...59

3.5. References……...62

Chapter 4: Conclusion and Future Directions……63

LIST OF TABLES

Table 3.1. PAMAM-amine and triethylamine react optimally with BCN-NHS in specific ratios, given as equivalents (eq.) in the table below. Mass (g), molecular weight (M.W.), moles, concentration, and volume are given for synthesizing approximately 1 mL of BCN solution.……56

LIST OF FIGURES

Figure 1.1. A depiction of (A) ionic crosslinking and (B) covalent crosslinking in alginate hydrogels. [72]……10

Figure 1.2. A schematic for the strain promoted alkyne-azide cycloaddition (SPAAC) reaction. The strained alkyne (reactant 2) spontaneously reacts with the azide (reactant 1) to form a stable triazole ring (product) [87]……...….12

Figure 2.1. Schematic for the erlotinib prodrug synthesis reaction…….….35

Figure 2.2. Proton nuclear magnetic resonance spectrograph confirming erlotinib prodrug structure……...36

Figure 2.3. Carbon-13 nuclear magnetic resonance spectrograph confirming erlotinib prodrug structure…….37

Figure 2.4. The structure of the erlotinib prodrug as analyzed by ChemDraw……....37

Figure 2.5. Chromatograph of standard erlotinib at its maximum absorbance of 346 nm……...39

Figure 2.6. Chromatograph of erlotinib prodrug at standard erlotinib's maximum absorbance of 346 nm……39

Figure 2.7. Nanodrop spectrograph of the erlotinib prodrug……40

Figure 2.8. Schematic for the reaction of erlotinib release from the erlotinib prodrug by hydrolysis……..41

Figure 2.9. Release of erlotinib prodrug over time……...41

Figure 2.10. The kinetics of the erlotinib prodrug represented by a semi-log plot……...42

Figure 3.1. The effect of NMP concentration on A431s after 48 hours of incubation. The EC_{50} was determined to be 0.32% NMP for this cell line……...54

Figure 3.2. The schematic for the 96-well plate used for assessing the cytotoxicity of the erlotinib prodrug. "Cells + NMP" refers to cells incubated with 0.2% NMP in media, "cells only" refers to cells incubated in DMEM media alone, and "media only" refers to wells containing only media and no cells……54

Figure 3.3. Graph representing the effects of standard erlotinib and the erlotinib prodrug after 48 hours as determined by a CCK-8 assay……..55

Figure 3.4. Reaction for synthesizing t-BCN. The four-armed PAMAM dendrimer reacts with BCN-NHS to yield a tetramer of BCN in a single step. T-BCN can then be purified by preparatory HPLC……...56

Figure 3.5. A picture of the t-BCN gels containing erlotinib prodrug and 24 hours of gelation……..57

Figure 3.6. Chromatograph of erlotinib released from prodrug-containing t-BCN hydrogels at the 36-hour time point (346 nm). The green line indicates the standard erlotinib control, the red line indicates the prodrug control, and the blue line indicates the sampled release buffer from a prodrug-containing hydrogel…….58

Figure 3.7. Chromatograph of erlotinib released from prodrug-containing t-BCN hydrogels at the five-day (120 hour) time point (346 nm). The blue line indicates the standard erlotinib control, the green line indicates the prodrug control, and the red line indicates the sampled release buffer from a prodrug-containing hydrogel……...……58

Chapter 1: Introduction

1.1 Current Limitations of Chemotherapeutics Used for the Treatment of Solid Tumors

Despite decades of research and the development of many novel treatments, cancer remains a leading cause of death worldwide and a major cause of diminished quality of life [1]. New discoveries and reformulations of chemotherapy drugs has led to an increase in the survival rates of cancer as a whole; however, several types of cancer, such as brain, liver, and pancreatic cancer, have had little to no significant improvements in survival [2, 3]. There are a variety of factors that contribute to the lack of efficacy in these cancer types, including the accessibility of the malignancy [4, 5], tumor characteristics such as aggressiveness [6], and the toxic side effects associated with chemotherapy administration [6, 7].

Current chemotherapies are severely limited by narrow therapeutic windows, wherein a potentially effective drug cannot be administered in the dosage necessary for treatment, as systemic distribution yields insufficient quantities of drug to the target site while simultaneously producing toxic off-target effects [7]. Furthermore, fast clearance rates necessitate repeated administration of large drug dosages in order to provide a consistent presence of drug to the target site [8]. This combination of limited therapeutic efficacy and off-target toxicity can be in large part attributed to poor drug delivery [1, 9]. Therefore, it is of great importance that novel, efficacious, and nontoxic methods of drug delivery are developed for the treatment of solid malignancies.

1.2 Drug Delivery Strategies

Current methods of delivering chemotherapy drugs to a target site overwhelmingly rely on systemic routes of administration, such as intravenous injections or oral administration [8, 9]. Drugs in systemic circulation are delivered to unnecessary locations and have the potential to cause off-target effects that greatly limit the therapeutic window and necessitate repeated doses [10]. Furthermore, drugs can be eliminated from the body through renal and nonrenal pathways before the drug is able to exert an effect [8]. It is therefore critical to develop strategies that overcome these barriers of drug delivery to target cancer sites. Approaches to improved drug delivery that are frequently used include chemical alteration of drugs to synthesize prodrug formulations, utilizing nanocarriers, and designing implantable drug depots.

1.2.1 Prodrugs

A prodrug is a compound that consists of a drug that is conjugated to a promoiety [11]. The addition of a promoiety prevents the drug from becoming pharmacologically active until that promoiety undergoes an enzymatic or chemical transformation that releases the drug in its active form [11, 12]. Prodrugs are common in the pharmaceutical industry and in clinical use, as they can be developed to alter a drug's solubility [13], increase chemical stability [14], improve diffusion [14, 15], and enhance tissue targeting [14, 16]. The overall goal that prodrug synthesis aims to achieve is the development of a stable compound with high bioavailability and reduced toxicity [11, 17].

This strategy has been successful at reducing the toxic side effects of cancer drugs that hinder efficacy. For example, the drug doxorubicin has established efficacy for treating a variety of sarcomas, but it's chemotherapeutic potential is limited by its serious adverse effects [18, 19].

Doxorubicin inhibits cancer growth by binding to DNA complexes and intercalating the DNA's double helix. This results in the cessation of DNA replication, thus preventing cell proliferation in both healthy and malignant tissues [18, 20, 21]. Additionally, doxorubicin is non-specific and capable of disrupting mitochondria function [22, 23]. This effect is evident in cardiomyocytes, the cell type in which mitochondria are most abundant, and ultimately results in dose-dependent cardiotoxicity [23, 24]. Doxorubicin diffuses quickly into tissues post-infusion, having a distribution half-life of just 3-5 minutes. Rapid diffusion into non-specific tissues prevents accumulation of doxorubicin at the target site and causes the array of adverse effects seen with doxorubicin administration [18]. The targeting ability and toxicity profile of doxorubicin could be improved by creating a prodrug formulation, and Kratz et al. accomplished this through conjugation of an acid-cleavable linker to doxorubicin. This doxorubicin derivative, named Aldoxorubicin (Aldox), rapidly and selectively binds to circulating albumin proteins [25]. Albumin has long been recognized for its utility as a drug carrier due to its tendency to accumulate in the tumor microenvironment [26, 27]. As such, intravenously administered Aldox binds to circulating albumin and accumulates in the tumor microenvironment, whose acidic properties lead to cleavage of the linker and release of free doxorubicin at the target site [28]. Circulating Aldox, particularly when bound to albumin, does not exert the toxic effect of doxorubicin and therefore reduces cardiotoxicity. In vivo studies confirmed this, demonstrating significantly reduced toxicity for Aldox as compared to free doxorubicin, with no significant difference in the antineoplastic effect [25, 29]. The attachment of an acid-cleavable linker that readily binds albumin resulted in a significantly wider therapeutic window, meaning that more drug can be administered, leading to a more potent antineoplastic effect [25, 28, 29].

There are drawbacks to the chemical modification strategy for cancer treatment: first, it is challenging to develop a prodrug with an ideal pharmacologic profile. Such a profile would include properties such as stability that allows the prodrug to reach the target site [16, 17], appropriate solubility [13], minimal off-target pathways [16, 17], low levels of active drug entering circulation, non-reactivity to non-target tissue components [11], persists for an appropriate duration for transformation, and favorable safety profiles of both the prodrug and the released promoiety [14]. Second, prodrugs that release drug through an enzymatic reaction necessitate the identification of a cancer-specific enzyme that is expressed at sufficient levels to allow for therapeutically relevant release of active drug. While many cancers over-express certain proteins or express mutated versions of normal proteins that could serve as targets, healthy tissues often express the same or similar proteins, which has potential for causing off-target effects [11, 16, 30]. Finally, while the chemical transformation strategy for release of prodrug may reduce off-target effects, systemic circulation of prodrug reduces the control over drug release and active drug may still be in circulation unnecessarily [17, 31]. Overall, systemic distribution is often part of the prodrug-based strategies, and a potential for off-target effects still exists.

1.2.2 Nanocarriers

Nanocarriers are drug delivery systems that consist of particles that are generally less than 500 nanometers in diameter [32]. The drug to be carried can be encapsulated by a shell of particles, or it can be covalently attached to the surface of particles. Encapsulation protects the drug from degradation and facilitates its transport regardless of its solubility, while surface presentation of drug can provide stability for targeting to take place [33]. As a whole, nanocarriers can offer increased stability, increased specificity, reduced toxicity, and improved

bioavailability and delivery of drugs [34]. Materials used for synthesizing nanocarriers include organic, inorganic, and hybrid materials with a wide variety of sizes, shapes, solubilities, and surface properties that impact the carrier's *in vivo* distribution [32, 34]. Some of the most commonly researched materials include liposomes and gold nanoparticles.

Liposomes, in the context of drug delivery, consist of an aqueous core enclosed by lipid bilayer(s) [35]. Such composition results in a biodegradable transporter that is also biocompatible and has low immunogenicity [35, 36]. Furthermore, both hydrophilic and lipophilic drugs are capable of being carried by lysosomes due to the aqueous core and lipid bilayer, respectively [8, 36]. Lysosomes deliver its payload through either passively diffusing to cells or through active transport into cells. Active transport mechanisms require the addition of targeting molecules on the surface of lysosomes, and this has been the approach of recent generations of lysosome carriers. Additional surface modifications, such as the addition of PEG molecules, are often made to mitigate a major limitation of liposome-based delivery approaches: reduced half-life in blood and tendency to be cleared by the reticuloendothelial system (RES) [36, 37]. However, there is difficulty in binding ligands to the surfaces of liposomes as there are few available surface groups and the potential for steric hinderance [38]. Yet, liposomes continue to be explored for a variety of uses across the field of drug delivery; in the case of chemotherapy delivery, there is some success, with several FDA-approved liposome-based chemotherapies currently on the market [37].

Gold nanoparticles have attracted a lot of attention in research due to its flexibility in design, reproducibility, low toxicity, and stability over a wide range of pH and temperatures [39, 40]. These nanoparticles are easily conjugated to biomolecules and readily undergo surface modifications that can lead to functionalization. Such surface modifications allow for the

nanoparticles to reliably evade the RES and prevent elimination before drug delivery can occur [41]. This ability to evade elimination also serves as a potential limitation of gold nanoparticles, since gold nanoparticles are non-biodegradable [39]. Furthermore, there are many inconsistencies in the research literature regarding the *in vivo* characteristics of gold nanoparticles [39, 41]. Full elucidation of characteristics such as biocompatibility, biodistribution, and clearance/elimination is needed.

There are limitations to the nanocarrier-drug delivery approach for cancer treatment. First, nanocarriers that aim to actively deliver a drug to a particular site require an established and specific target. As mentioned previously, creating a drug or drug carrier that is chemically stable, biocompatible, efficacious, and active at a specific target site is difficult to achieve when delivered systemically. Second, nanocarriers using passive mechanisms for delivery, including those constructed to accumulate or aggregate within the tumor microenvironment, are constructed to utilize the proposed "enhanced permeability and retention (EPR) effect" [32, 42]. The EPR effect theory states that, due to the combination of defective "leaky" vasculature and low-functioning or absent lymphatics often observed in solid tumors, molecules and particles are able to pass into the tumor microenvironment and evade clearance [43]. Many delivery strategies utilizing nanocarriers are contingent upon the validity of the EPR effect; unfortunately, studies have failed to provide evidence for this effect being consistent across different tumors [44, 45, 46]. As such, a clearer understanding of the mechanisms involved in nanocarrier delivery to tumor sites is needed. Nonetheless, decades of research have produced a myriad of nanocarrier-based delivery strategies for improving chemotherapy, but these strategies overwhelmingly fail to be translated into clinical use [45]. While research and development of these systems has no

doubt produced valuable information and a few major discoveries, the issue of effective delivery of chemotherapeutics to solid tumor sites persists.

1.2.3 Drug Depots

Currently used chemotherapeutics could be delivered to a target site in higher, more effective doses while diminishing off-target toxicity if the drug is delivered locally rather than through systemic circulation. Local presentation of drug is achievable through implantable drug-eluting depots. Drug depots are devices implanted into the body for the purpose of controlled drug release [47]. These drug-eluting devices have clinical significance, exhibiting utility as stents for cardiovascular conditions [48], implantable hormonal contraceptives [49], and cancer therapies [50].

One such example of a drug depot for chemotherapeutic delivery is Gliadel, which is used for the treatment of an aggressive form of brain cancer called glioblastoma [50]. Gliadel is used as an adjunct therapy to surgery and consists of the chemotherapy drug carmustine contained within a polymer disc [50, 51]. Surgical debulking of glioblastoma tumors results in "dirty margins," wherein tumor cells remain among healthy tissue because attempting to remove them would result in substantial sacrifice of healthy brain tissue [52]. After the surgical debulking of a glioblastoma tumor, Gliadel wafers are placed on the walls of the surgical cavity. Placement of these wafers into the tumor bed has the advantage of by-passing the blood brain barrier and provides high concentrations of carmustine directly [51, 53]. This adjunct therapy results a statistically significant increase in survival time of approximately 3 months [50, 51, 54]. However, this approach to drug depots has several limitations; first, drug persistence is limited by rapid depletion of the drug cargo from the depot. The majority of carmustine elutes from the

polymer depot over a period of five days and persists in brain tissue for only one week [50, 53, 55]. Second, the depot can only be placed as an adjunct to surgery. Patients with non-resectable tumors are not eligible for this treatment and placing more depots once the wafers degrade is not feasible, as this would necessitate further surgery [53, 56]. Finally, carmustine exits the wafer in a burst release, wherein much of the drug elutes from the depot within the first 24 hours after placement. A burst release limits the amount of drug that can be loaded into a depot, as the addition of more drug into the depot for the purposes of extending the elution time could result in uncontrolled tissue toxicity [57].

The success of Gliadel as one of the only pharmaceutical treatments available for glioblastoma is an indication that drug depots could be the drug delivery system that offers localized, sustained, and controlled release of chemotherapy, ultimately improving treatment outcomes. It's limitations, however, reveal the need to further develop depot systems for the treatment of cancer. In particular, this strategy could be improved by manufacturing a depot that prolongs drug exposure, offers a stable rate of drug release, and can be placed in the body in a minimally invasive way.

1.3. Hydrogels as Drug Delivery Systems

Among the multitude of proposed drug delivery systems for controlled delivery, hydrogels stand out as an ideal candidate for improving chemotherapeutic delivery due to their high biocompatibility, flexibility, modifiable mechanical properties, tunable degradation rates, and adjustable porosity. A hydrogel is a highly hydrated 3-dimensional network of crosslinked polymers, and they are commonly used many areas of biomedical engineering for a variety of

applications, including tissue engineering and pharmacoengineering. The specific chemical and physical properties of a hydrogel depend in large part on the polymer material used. Synthetic hydrogels, such as PLGA and PEG, offer enhanced gel strength and increased chemical and mechanical reproducibility. However, naturally occurring polymers, such as collagen or alginate, have the advantage of innate biocompatibility. With there being greater focus on designing biomaterials that functionally simulate the extracellular environment within a given tissue, nature-derived polymers have regained attention within the bioengineering research community. A major advantage that hydrogels as a whole offer in terms of delivery strategies is their mechanical properties allow permit depot placement via injection. This is minimally invasive compared to surgical placement. The ideal polymer for hydrogel development is highly dependent on what the hydrogel is supposed to do and where it is to be placed.

1.3.1. Alginate-based Hydrogels

Alginate is an anionic polysaccharide most often derived from brown algae that is frequently used in biomedical engineering due to its low toxicity, chemical versatility, low immunogenicity, and high biocompatibility. Hydrogels composed of alginate exhibit structural similarities to the extracellular matrix of many tissues, a characteristic which has led to its use in applications such as wound dressings, cell culturing, and drug delivery.

Alginates are composed of alginic acid, a linear copolymer composed of covalently linked residues of α-L-guluronic acid and 1,4-linked β-D-mannuronic acid. Both guluronic acid and mannuronic acid can covalently link in homopolymeric sections (“G blocks” and “M blocks,” respectively) and in heteropolymeric sections. The ratio of M/G residues and the arrangement of these blocks affects the alginate’s properties, such as affinity towards ions and

viscosity, that will ultimately determine the final properties of the alginate-material and its potential applications. For example, alginates with a higher composition of G blocks produce stiffer, more stable hydrogels. Additionally, G blocks are mostly responsible for typical strategy for crosslinking alginate: G blocks on separate strands of alginate associate with each other in the presence of divalent cations like calcium ions (Ca^{2+}) through ionic bonds, producing an "egg box" structure (Grant et al 1973). Gelation can also occur through covalent interactions with the available functional groups (-OH, $-NH_2$, -COOH), but it occurs most commonly with the carboxylic groups. Regardless of the method of gelation, the rate of gelation depends on several variables, including temperature, pH, the ratio of M/G residues, the crosslinking agent used, and the presence of other compounds. Overall, alginate gel formation occurs under neutral conditions with non-toxic reactants.

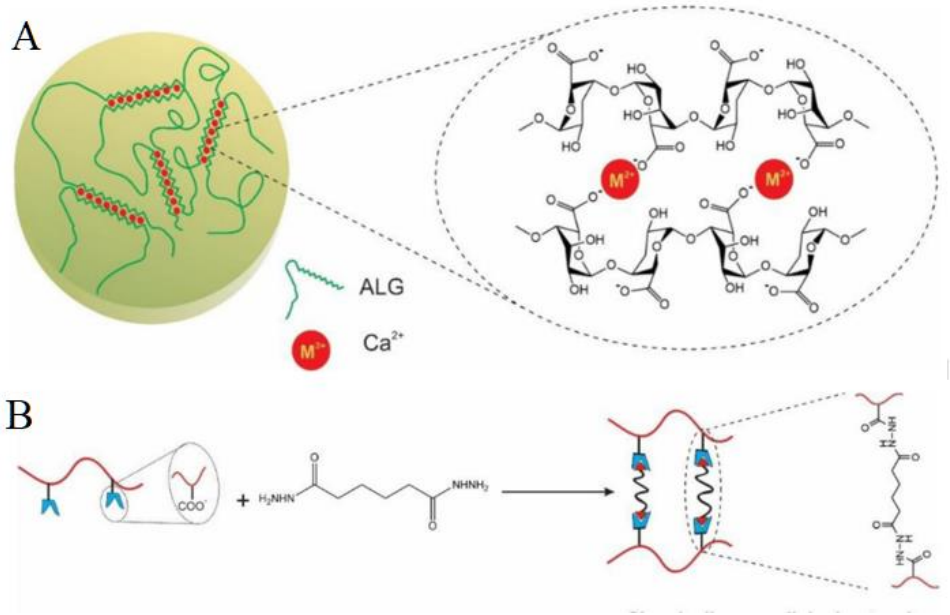

Figure 1.1. A depiction of (A) ionic crosslinking and (B) covalent crosslinking in alginate hydrogels. [72]

Due to its non-immunogenicity, non-toxicity, high-water content, pH sensitivity, and ease of chemical modification due to available functional groups, alginate hydrogels make ideal candidates for drug delivery depots. As Fenn et al. demonstrated, alginate hydrogels can be used as a drug delivery vehicle for delivering doxorubicin to lung cancer cells. First, a solution containing alginate, methacrylate, and doxorubicin was subjected to water/oil emulsion to doxorubicin-containing sub-microspheres. Next, the sub-microspheres were photo-crosslinked with methacrylate, which utilized alginate's available hydroxyl groups to form covalent bonds. Then, the sub-microspheres were further crosslinked with calcium chloride, which utilized alginate's carboxyl groups on neighboring alginate strands. The result was dually crosslinked doxorubicin-containing alginate sub-microspheres. These sub-microspheres were incubated with a human's lung cancer cell line, A549, and cellular uptake and drug delivery efficacy were assessed. Greater than 80% of the added sub-microspheres were taken up by the cells, and mitochondrial activity was greatly reduced by diffused doxorubicin in treated cells within 24 hours. Blank sub-microspheres were internalized but had no effect on mitochondrial activity. Overall, clinically relevant doses of doxorubicin were successfully delivered to A549s in a controlled manner. With the potential for localized injection directly to a cancer site, there is promise for alginate hydrogels as a drug delivery system.

1.3.2. Click Chemistry and Hydrogels

"Click chemistry" refers to chemical reactions which are spontaneous, rapid, extremely selective, are stable in a physiological environment, do not result in toxic byproducts, produce high yields, and react under mild conditions. Click chemistry has been used as a method for

crosslinking to rapidly produce stable hydrogels with increased mechanical strength. For example, Gao et al. developed an injectable PEG-based hydrogel containing doxorubicin using a thiol-ene click reaction. The resulting hydrogel could form *in situ*, was biodegradable, and released doxorubicin in a sustained fashion. While the drug-free click-based hydrogels exhibited no toxicity, hydrogels containing doxorubicin were effective in producing a cytotoxic effect.

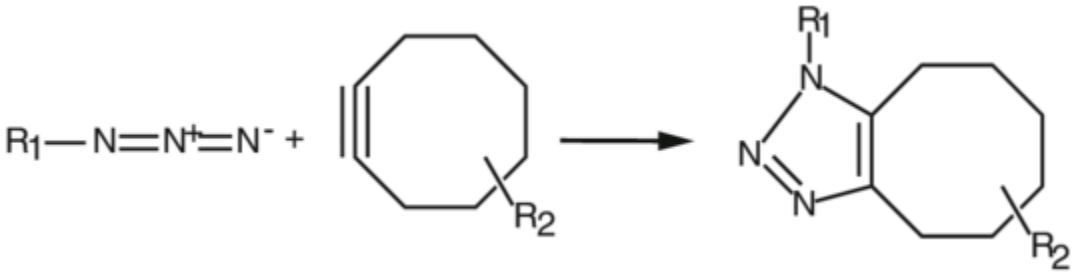

Figure 1.2. A schematic for the strain promoted alkyne-azide cycloaddition (SPAAC) reaction. The strained alkyne (reactant 2) spontaneously reacts with the azide (reactant 1) to form a stable triazole ring (product) [87].

The term "click chemistry" encompasses several types of reactions, but strain promoted alkyne-azide cycloadditions (SPAAC) in particular has been attracting attention for its utility in bioconjugation. In a SPAAC reaction, an azide and an alkyne-containing cyclooctyne spontaneously react to produce an inert triazole ring. This reaction has the capacity to functionalize alginate hydrogels for improved drug delivery. This is evident in a publication by Brudno et al.: SPAAC was used to bond circulating prodrugs to implanted hydrogels *in vivo.* This resulted in capture-and-release system that captured circulating cyclooctyne-modified prodrugs within the azide-modified alginate hydrogel. Upon reaction of the cyclooctyne and azide, the active drug is released and able to exert its effects locally. As such, the alginate hydrogel drug depot becomes "refillable," capable of releasing multiple payloads over time. Moody et al. further demonstrated the utility of this reaction through improving the *in vivo*

stability of capture-and-release alginate-based hydrogels. Alginate strands were modified to display azides and the typically used calcium-based crosslinker was replaced with a cyclooctyne. The resulting SPAAC reaction covalently crosslinked the alginate strands, producing a hydrogel. Some azides remained available within the gel, which could be used to capture cyclooctyne-modified prodrugs within the aforementioned refillable drug delivery system. Ultimately, click chemistry shows significant promise in hydrogel synthesis due to its capacity for functionalization, its biocompatibility, its specificity, and the rapidly produced high yields.

1.4. Research Objectives

Tremendous amounts of research effort has gone into developing methods to reduce the toxicity and increase the efficacy of chemotherapy drugs. Localized drug delivery depots show promise, with hydrogel-based systems attracting a lot of attention. There have been many studies that investigated the utility of alginate hydrogels for drug delivery. However, the strategies undertaken in these studies are limited by a variety of factors, including the crosslinker used in the gels, the method of drug release, the gel's drug binding repertoire.

As stated previously, there are two methods for crosslinking: ionic and covalent. Ionic crosslinking is more commonly used in hydrogel production, but this method of crosslinking causes poorly controlled gelation rates and results in gels that are ultimately unstable due to gradual release of the divalent cations. Loss of the crosslinking agent leads to the breakdown of the gel within the body and presents the possibility of an elevated immune response. Alternatively, covalent crosslinking allows for tightly controlled degradation rates and mechanical properties [65]. The method by which loaded drugs are released is an important

consideration. Drugs that are loaded into the gels through ionically interacting with alginate will release by diffusion. Drug release by diffusion in this way quickly expends the payload of the gel, similar to the release of carmustine in Gliadel wafers. Diffusive drug release is also poorly controlled [82]. A chemically controlled release mechanism would offer control over release rates, potentially through utilization of covalent coupling. Furthermore, while it is often noted that the chemical characteristics of a drug are important when considering incorporation into a hydrogel, most studies do not focus on creating a hydrogel system that is compatible with a wide variety of drugs, regardless of chemical properties. An advantage that alginate offers is its chemical versatility and potential for modification; this advantage is often utilized to modify hydrogels for delivery of specific drugs, but there has been limited investigation into developing a delivery system that can be easily modified to bind drugs with differing chemical properties.

The goal of this research is to address these limitations by creating a drug delivery system that releases targeting chemotherapy drugs locally in a controlled, tunable fashion. This system would ideally be chemically stable, biocompatible, compatible with a variety of drugs, have tunable release rates, and is minimally invasive. Click chemistry-based alginate hydrogels meet the criteria for this system and have demonstrated efficacy in previous studies.

For proof-of-concept, a chemotherapy drug must be selected and modified to bind to this hydrogel. Many studies use doxorubicin, but this drug is nonspecific and is highly toxic to healthy tissues [83]. To minimize off-target toxicity, a target-specific drug that is applicable to many cancer types is ideal. For this reason, EGFR-inhibition was selected as the target mechanism. The epidermal growth factor receptor (EGFR) family consists of transmembrane receptors that, when activated, trigger an intracellular cascade that results in the activation of transcription factors that ultimately lead to DNA synthesis and cell proliferation [84]. EGFR is

expressed in many healthy tissues; however, in many cancer types, including certain lung cancers, epithelial cancers, and glioblastoma, EGFR is overexpressed. In some cases, EGFR can become mutated to be constitutively active, providing constant signaling that leads to uncontrolled cell proliferation [84, 85]. Certain tyrosine kinase inhibitors are used as chemotherapeutics that can bind EGFR and prevent it from signaling. This slows or halts cancer progression [86]. For the following research, the tyrosine kinase inhibitor erlotinib is modified with a linker to form a "prodrug" version of erlotinib that can participate in click chemistry reactions, allowing it to bind to a click-modified alginate hydrogel. Altogether, the purpose of this dissertation is to provide proof-of-concept for a biocompatible injectable hydrogel drug delivery system that allows controlled, sustained, and localized drug release for the improved treatment of cancer.

1.6 References

1. Hu, Q., Sun, W., Wang, C., & Gu, Z. (2016). Recent advances of cocktail chemotherapy by combination drug delivery systems. *Advanced drug delivery reviews*, *98*, 19–34. doi: 10.1016/j.addr.2015.10.022

2. Allemani, C., Matsuda, T., Di Carlo, V., Harewood, R., Matz, M., Nikšić, M., Bonaventure, A., Valkov, M., Johnson, C. J., Estève, J., Ogunbiyi, O. J., Azevedo E Silva, G., Chen, W. Q., Eser, S., Engholm, G., Stiller, C. A., Monnereau, A., Woods, R. R., Visser, O., Lim, G. H., Aitken, J., Weir, H. K., Coleman, M. P., & CONCORD Working Group. (2018). Global surveillance of trends in cancer survival 2000-14 (CONCORD-3): analysis of individual records for 37 513 025 patients diagnosed with one of 18 cancers from 322 population-based registries in 71 countries. *Lancet, 391*(10125), 1023–75. doi: 10.1016/S0140-6736(17)33326-3

3. Jemal, A., Ward, E. M., Johnson, C. J., Cronin, K. A., Ma, J., Ryerson, B., Mariotto, A., Lake, A. J., Wilson, R., Sherman, R. L., Anderson, R. N., Henley, S. J., Kohler, B. A., Penberthy, L., Feuer, E. J., & Weir, H. K. (2017). Annual Report to the Nation on the Status of Cancer, 1975-2014, Featuring Survival. *Journal of the National Cancer Institute, 109*(9). doi: 10.1093/jnci/djx030

4. Brem, H., Piantadosi, S., Burger, P. C., Walker, M., Selker, R., Vick, N. A., Black, K., Sisti, M., Brem, S., Mohr, G., Muller, P., Morawetz, R., & Schold, S.C. (1995). Placebo-controlled trial of safety and efficacy of intraoperative controlled delivery by biodegradable polymers of chemotherapy for recurrent gliomas. The Polymer-brain Tumor Treatment Group. *Lancet, 345*(8956), 1008-12. doi: 10.1016/s0140-6736(95)90755-6

5. Indolfi, L., Ligorio, M., Ting, D. T., Xega, K., Tzafriri, A. R., Bersani, F., Aceto, N., Thapar, V., Fuchs, B. C., Deshpande, V., Baker, A. B., Ferrone, C. R., Haber, D. A., Langer, R., Clark, J. W., & Edelman, E. R. (2016). A tunable delivery platform to provide local chemotherapy for pancreatic ductal adenocarcinoma. *Biomaterials, 93*, 71–82. doi: 10.1016/j.biomaterials.2016.03.044

6. Batchelor, T. T., Gerstner, E. R., Emblem, K. E., Duda, D. G., Kalpathy-Cramer, J., Snuderl, M., Ancukiewicz, M., Polaskova, P., Pinho, M. C., Jennings, D., Plotkin, S. R., Chi, A. S., Eichler, A. F., Dietrich, J., Hochberg, F. H., Lu-Emerson, C., Iafrate, A. J., Ivy, S. P., Rosen, B. R., Loeffler, J. S., Wen, P. Y., Sorensen, A. G., & Jain, R. K. (2013). Improved tumor oxygenation and survival in glioblastoma patients who show increased blood perfusion after cediranib and chemoradiation. *PNAS, 110* (47), 19059-64. doi: 10.1073/pnas.1318022110

7. Lotfi-Jam, K., Carey, M., Jefford, M., Schofield, P., Charleson, C., & Aranda, S. (2008). Nonpharmacologic strategies for managing common chemotherapy adverse effects: a systematic review. *Journal of Clinical Oncology, 26*(34), 5618-29. doi: 10.1200/JCO.2007.15.9053

8. Laffleur, F., & Keckeis, V. (2020). Advances in drug delivery systems: Work in progress still needed?. *International journal of pharmaceutics: X, 2*, 100050. doi: 10.1016/j.ijpx.2020.100050

9. Anaya, D. A., Dogra, P., Wang, Z., Haider, M., Ehab, J., Jeong, D. K., Ghayouri, M., Lauwers, G. Y., Thomas, K., Kim, R., Butner, J. D., Nizzero, S., Ramírez, J. R., Plodinec, M., Sidman, R. L., Cavenee, W. K., Pasqualini, R., Arap, W., Fleming, J. B., &

Cristini, V. (2021). A Mathematical Model to Estimate Chemotherapy Concentration at the Tumor-Site and Predict Therapy Response in Colorectal Cancer Patients with Liver Metastases. *Cancers, 13*(3), 444-62. doi: 10.3390/cancers13030444

10. Sun T., Zhang Y. S., Pang B., Hyun D. C., Yang M., Xia Y. (2014). Engineered nanoparticles for drug delivery in cancer therapy. *Angewandte Chemie, 53,* 12320–64. doi: 10.1002/anie.201403036

11. Vale, N., Ferreira, A., Matos, J., Fresco, P., & Gouveia, M. J. (2018). Amino acids in the development of prodrugs. *Molecules*, *23*(9), 2318-79. doi: 10.3390/molecules23092318

12. Jornada, D. H., Fernandes, G. F., Chiba, D. E., Ferreira de Melo, T. R., Leandro dos Santos, J., & Chung, M. C. (2016). The prodrug approach: a successful tool for improving drug solubility. *Molecules, 21*(1), 42-73. doi: 10.3390/molecules21010042

13. Stella V. J. & Nti-Addae, K. W. (2007). Prodrug strategies to overcome poor water solubility. *Advanced Drug Delivery Reviews, 59*(7), 677–94. doi: 10.1016/j.addr.2007.05.013

14. Lin, C., Sunkara, G., Cannon, J. B., & Ranade, V. (2012). Recent advances in prodrugs as drug delivery systems. *American Journal of Therapeutics*, *19*(1), 33-43. doi: 10.1097/MJT.0b013e3181f47f3f

15. Huttunen, K. M. & Rautio, J. (2011). Prodrugs - an efficient way to breach delivery and targeting barriers. *Current Topics in Medicinal Chemistry, 11*(18), 2265-87. doi: 10.2174/156802611797183230

16. Mishra, A. P., Chandra, S., Tiwari, R., Srivastava, A., & Tiwari, G. (2018). Therapeutic Potential of Prodrugs Towards Targeted Drug Delivery. *Open Medicinal Chemistry Journal*, *23*(12), 111-23. doi: 10.2174/1874104501812010111

17. Delahousse, J., Skarbek, C. & Paci, A. (2019). Prodrugs as drug delivery system in oncology. *Cancer Chemotherapy and Pharmacology*, *84*, 937–58. doi: 10.1007/s00280-019-03906-2

18. Tacar, O., Sriamornsak, P., & Dass, C. R. (2013). Doxorubicin: an update on anticancer molecular action, toxicity and novel drug delivery systems. *Journal of Pharmacy and Pharmacology*, *65*(2), 157–70, doi: 10.1111/j.2042-7158.2012.01567

19. Mancilla, T. R., Iskra, B., & Aune, G. J. (2019). Doxorubicin-Induced Cardiomyopathy in Children. *Comprehensive Physiology*, *9*(3), 905–931. doi: 10.1002/cphy.c180017

20. Carvalho C, Santos RX, Cardoso S, Correia S, Oliveira PJ, Santos MS, Moreira PI. Doxorubicin: the good, the bad and the ugly effect. Curr Med Chem. 2009;16(25):3267-85. doi: 10.2174/092986709788803312. Epub 2009 Sep 1. PMID: 19548866.

21. Minotti G, Menna P, Salvatorelli E, Cairo G, Gianni L. Anthracyclines: molecular advances and pharmacologic developments in antitumor activity and cardiotoxicity. Pharmacol Rev. 2004 Jun;56(2):185-229. doi: 10.1124/pr.56.2.6. PMID: 15169927.

22. Gorini, S., De Angelis, A., Berrino, L., Malara, N., Rosano, G., & Ferraro, E. (2018). Chemotherapeutic Drugs and Mitochondrial Dysfunction: Focus on Doxorubicin, Trastuzumab, and Sunitinib. *Oxidative medicine and cellular longevity*, *2018*, 7582730. https://doi.org/10.1155/2018/7582730

23. Osataphan, N., Phrommintikul, A., Chattipakorn, S. C., & Chattipakorn, N. (2020). Effects of doxorubicin-induced cardiotoxicity on cardiac mitochondrial dynamics and mitochondrial function: Insights for future interventions. *Journal of cellular and molecular medicine, 24*(12), 6534–6557. https://doi.org/10.1111/jcmm.15305

24. Shi Y, Moon M, Dawood S, McManus B, Liu PP. Mechanisms and management of doxorubicin cardiotoxicity. Herz. 2011 Jun;36(4):296-305. doi: 10.1007/s00059-011-3470-3. PMID: 21656050.

25. Kratz F, Warnecke A, Scheuermann K, Stockmar C, Schwab J, Lazar P, Drückes P, Esser N, Drevs J, Rognan D, Bissantz C, Hinderling C, Folkers G, Fichtner I, Unger C. Probing the cysteine-34 position of endogenous serum albumin with thiol-binding doxorubicin derivatives. Improved efficacy of an acid-sensitive doxorubicin derivative with specific albumin-binding properties compared to that of the parent compound. J Med Chem. 2002 Dec 5;45(25):5523-33. doi: 10.1021/jm020276c.

26. Sinn H, Schrenk HH, Friedrich EA, Schilling U, Maier-Borst W. Design of compounds having an enhanced tumour uptake, using serum albumin as a carrier. Part I. Int J Rad Appl Instrum B. 1990;17(8):819-27. doi: 10.1016/0883-2897(90)90031-u. PMID: 2079429.

27. Parodi, A., Miao, J., Soond, S. M., Rudzińska, M., & Zamyatnin, A. A., Jr (2019). Albumin Nanovectors in Cancer Therapy and Imaging. *Biomolecules*, *9*(6), 218. https://doi.org/10.3390/biom9060218

28. Cranmer LD. Spotlight on aldoxorubicin (INNO-206) and its potential in the treatment of soft tissue sarcomas: evidence to date. Onco Targets Ther. 2019;12:2047-2062 doi: 10.2147/OTT.S145539

29. Walker, L., Perkins, E., Kratz, F., & Raucher, D. (2012). Cell penetrating peptides fused to a thermally targeted biopolymer drug carrier improve the delivery and antitumor efficacy of an acid-sensitive doxorubicin derivative. *International journal of pharmaceutics*, *436*(1-2), 825–832. https://doi.org/10.1016/j.ijpharm.2012.07.043

30. Rautio, J., Meanwell, N., Di, L. *et al.* The expanding role of prodrugs in contemporary drug design and development. *Nat Rev Drug Discov* **17,** 559–587 (2018). https://doi.org/10.1038/nrd.2018.46

31. Mahato, R., Tai, W., & Cheng, K. (2011). Prodrugs for improving tumor targetability and efficiency. *Advanced drug delivery reviews*, *63*(8), 659–670. https://doi.org/10.1016/j.addr.2011.02.002

32. Din, F. U., Aman, W., Ullah, I., Qureshi, O. S., Mustapha, O., Shafique, S., & Zeb, A. (2017). Effective use of nanocarriers as drug delivery systems for the treatment of selected tumors. *International journal of nanomedicine*, *12*, 7291–309. doi: 10.2147/IJN.S146315

33. Grumezescu, A. M. (2019). *Nanomaterials for Drug Delivery and Therapy*. Elsevier, 1-51. ISBN 9780128165058

34. Koo, H., Huh, M. S., Sun, I. C., Yuk, S. H., Choi, K., Kim, K., & Kwon, I. C. (2011). In vivo targeted delivery of nanoparticles for theranosis. *Accounts of Chemical Research, 44*, 1018-28. doi: 10.1021/ar2000138

35. Manaia, E. B., Abuçafy, M. P., Chiari-Andréo, B. G., Silva, B. L., Oshiro Junior, J. A., & Chiavacci, L. A. (2017). Physicochemical characterization of drug nanocarriers. *International journal of nanomedicine, 12,* 4991–5011. doi: 10.2147/IJN.S133832

36. Pattni, B. S., Chupin V. V., & Torchilin, V. P. (2015). New Developments in Liposomal Drug Delivery. *Chemical Reviews, 115*(19), 10938-66. doi: 10.1021/acs.chemrev.5b00046

37. Deshpande, P. P., Biswas, S., & Torchilin, V.P. (2013). Current trends in the use of liposomes for tumor targeting. *Nanomedicine, 8*(9), 1509–28. doi: 10.2217/nnm.13.118

38. Kuai, R., Yuan, W., Qin, Y., Chen, H., Tang, J., Yuan, M., Zhang, Z., & He, Q. (2010). Efficient delivery of payload into tumor cells in a controlled manner by TAT and thiolytic cleavable PEG co-modified liposomes. *Molecular Pharmaceutics, 7*(5), 1816-26. doi: 10.1021/mp100171c

39. Mizuhara, T., Saha, K., Moyano, D. F., Kim, C. S., Yan, B., Kim, Y. K., & Rotello, V. M. (2015). Acylsulfonamide-Functionalized Zwitterionic Gold Nanoparticles for Enhanced Cellular Uptake at Tumor pH. *Angewandte Chemie (International ed. in English), 54*(22), 6567–70. doi: 10.1002/anie.201411615

40. Ruan, S., Yuan, M., Zhang, L., Hu, G., Chen, J., Cun, X., Zhang, Q., Yang, Y., He, Q., & Gao, H. (2015). Tumor microenvironment sensitive doxorubicin delivery and release to glioma using angiopep-2 decorated gold nanoparticles. *Biomaterials, 37,* 425-35. doi: 10.1016/j.biomaterials.2014.10.007

41. Zorkina, Y., Abramova, O., Ushakova, V., Morozova, A., Zubkov, E., Valikhov, M., Melnikov, P., Majouga, A., & Chekhonin, V. (2020). Nano Carrier Drug Delivery

Systems for the Treatment of Neuropsychiatric Disorders: Advantages and Limitations. *Molecules (Basel, Switzerland)*, *25*(22), 5294. doi: 10.3390/molecules25225294

42. Chen, B., Dai, W., He, B., Zhang, H., Wang, X., Wang, Y., & Zhang, Q. (2017). Current Multistage Drug Delivery Systems Based on the Tumor Microenvironment. *Theranostics*, *7*(3), 538–558. doi: 10.7150/thno.16684
43. Matsumura Y, Maeda H. (1986). A new concept for macromolecular therapeutics in cancer chemotherapy: mechanism of tumoritropic accumulation of proteins and the antitumor agent smancs. *Cancer Research, 46*(12 Pt 1), 6387-92.
44. Hansen, A. E., Petersen, A. L., Henriksen, J. R., Boerresen, B., Rasmussen, P., Elema, D. R., af Rosenschöld, P. M., Kristensen, A. T., Kjær, A., & Andresen, T. L. (2015). Positron Emission Tomography Based Elucidation of the Enhanced Permeability and Retention Effect in Dogs with Cancer Using Copper-64 Liposomes. *ACS Nanotechnology, 9*(7), 6985-95. doi: 10.1021/acsnano.5b01324
45. Thakor, A. S. & Gambhir, S. S. (2013). Nanooncology: the future of cancer diagnosis and therapy. *CA: A Cancer Journal for Clinicians, 63*(6), 395-418. doi: 10.3322/caac.21199
46. Wilhelm, S., Tavares, A., Dai, Q., Ohta, S., Audet, J., Dvorak, H. F., & Chan, W. C. W. (2016). Analysis of nanoparticle delivery to tumours. *Nature Reviews Materials, 1*, 16014. doi: 10.1038/natrevmats.2016.14
47. Kamaly, N., Yameen, B., Wu, J., & Farokhzad, O. C. (2016). Degradable Controlled-Release Polymers and Polymeric Nanoparticles: Mechanisms of Controlling Drug Release. *Chemical reviews*, *116*(4), 2602–2663. https://doi.org/10.1021/acs.chemrev.5b00346

48. Wessely R. New drug-eluting stent concepts. Nat Rev Cardiol. 2010 Apr;7(4):194-203. doi: 10.1038/nrcardio.2010.14. Epub 2010 Mar 2. PMID: 20195268.

49. Dinehart, E., Lathi, R. B., & Aghajanova, L. (2020). Levonorgestrel IUD: is there a long-lasting effect on return to fertility?. *Journal of assisted reproduction and genetics*, *37*(1), 45–52. https://doi.org/10.1007/s10815-019-01624-5

50. Xing, W. K., Shao, C., Qi, Z. Y., Yang, C., & Wang, Z. (2015). The role of Gliadel wafers in the treatment of newly diagnosed GBM: a meta-analysis. *Drug design, development and therapy*, *9*, 3341–3348. https://doi.org/10.2147/DDDT.S85943

51. Nagpal S. The role of BCNU polymer wafers (Gliadel) in the treatment of malignant glioma. Neurosurg Clin N Am. 2012 Apr;23(2):289-95, ix. doi: 10.1016/j.nec.2012.01.004. Epub 2012 Feb 18. PMID: 22440872.

52. Gaspar LE, Fisher BJ, Macdonald DR, LeBer DV, Halperin EC, Schold SC Jr, Cairncross JG. Supratentorial malignant glioma: patterns of recurrence and implications for external beam local treatment. Int J Radiat Oncol Biol Phys. 1992;24(1):55-7. doi: 10.1016/0360-3016(92)91021-e. PMID: 1512163.

53. Fleming, A.B., Saltzman, W.M. Pharmacokinetics of the Carmustine Implant. *Clin Pharmacokinet* **41,** 403–419 (2002). https://doi.org/10.2165/00003088-200241060-00002

54. Chaichana KL, Zaidi H, Pendleton C, et al. The efficacy of carmustine wafers for older patients with glioblastoma multiforme: prolonging survival. Neurol Res. 2011;33(7):759–764

55. Azizi SA, Miyamoto C. Principles of treatment of malignant gliomas in adults: an overview. J Neurovirol 1998; 4(2): 204–16

56. Tew K, Colvin OM, Chabner BA. Alkylating agents. In: Chabner BA, Longo DL, editors. Cancer chemotherapy and biotherapy. Chapter 12. Philadelphia (PA): Lippincott-Raven Publishers, 1991: 297–332

57. Han, D., Serra, R., Gorelick, N., Fatima, U., Eberhart, C. G., Brem, H., Tyler, B., & Steckl, A. J. (2019). Multi-layered core-sheath fiber membranes for controlled drug release in the local treatment of brain tumor. *Scientific Reports*, **9,** 17936. doi: 10.1038/s41598-019-54283-y

58. Bashir, S., Hina, M., Iqbal, J., Rajpar, A. H., Mujtaba, M. A., Alghamdi, N. A., Wageh, S., Ramesh, K., & Ramesh, S. (2020). Fundamental Concepts of Hydrogels: Synthesis, Properties, and Their Applications. *Polymers*, *12*(11), 2702. doi: 10.3390/polym12112702

59. Bahram, M., Mohseni, N., & Moghtader, M. (2016). An Introduction to Hydrogels and Some Recent Applications, Emerging Concepts in Analysis and Applications of Hydrogels. Sutapa Biswas Majee, IntechOpen, doi: 10.5772/64301

60. Biswas G., Majee S., & Roy A. (2016). Combination of synthetic and natural polymers in hydrogel: An impact on drug permeation. *Journal of Applied Pharmaceutical Science, 6,* 158–164. doi: 10.7324/JAPS.2016.601125

61. Karoyo, A. H., & Wilson, L. D. (2021). A Review on the Design and Hydration Properties of Natural Polymer-Based Hydrogels. *Materials (Basel, Switzerland), 14*(5), 1095. doi: 10.3390/ma14051095

62. Chimisso, V., Aleman Garcia, M. A., Yorulmaz Avsar, S., Dinu, I. A., & Palivan, C. G. (2020). Design of Bio-Conjugated Hydrogels for Regenerative Medicine Applications:

From Polymer Scaffold to Biomolecule Choice. *Molecules (Basel, Switzerland)*, *25*(18), 4090. doi: 10.3390/molecules25184090

63. Ibeanu, N., Egbu, R., Onyekuru, L., Javaheri, H., Khaw, P. T., Williams, G. R., Brocchini, S., & Awwad, S. (2020). Injectables and Depots to Prolong Drug Action of Proteins and Peptides. *Pharmaceutics*, *12*(10), 999. doi: 10.3390/pharmaceutics12100999
64. George, M. & Abraham, T. E. (2006). Polyionic hydrocolloids for the intestinal delivery of protein drugs: alginate and chitosan--a review. *Journal of Controlled Release*, *114*(1), 1-14. doi: 10.1016/j.jconrel.2006.04.017
65. Lee, K. Y., & Mooney, D. J. (2012). Alginate: properties and biomedical applications. *Progress in polymer science*, *37*(1), 106–126. doi: 10.1016/j.progpolymsci.2011.06.003
66. Jain, D. & Bar-Shalom, D. (2014). Alginate drug delivery systems: application in context of pharmaceutical and biomedical research. *Drug Development and Industrial Pharmacy*, *40*(12), 1576-84. doi: 10.3109/03639045.2014.917657
67. Hay, I. D., Rehman, Z. U., Ghafoor, A., & Rehm, B. H. A. (2010). Bacterial biosynthesis of alginates. *Journal of Chemical Technology & Biotechnology*, *85*, 752–759. doi: 10.1007/s002530051051
68. Grant, G. T., Morris, E. R., Rees, D. A., Smith, P. J. C., & Thom, D. (1973). Biological interactions between polysaccharides and divalent cations - egg-box model. *FEBS Letters*, *32*, 195–198. doi: 10.1016/0014-5793(73)80770-7
69. Draget, K. I., Skjåk Bræk, G., & Smidsrød, O. (1994). Alginic acid gels: the effect of alginate chemical composition and molecular weight. *Carbohydrate Polymers*, *25*(1), 31–38. doi: 10.1016/0144-8617(94)90159-7

70. Szekalska, M., Pucilowska, A., Szymanska, E., & Ciosek, P. (2016). Alginate: Current Use and Future Perspectives in Pharmaceutical and Biomedical Applications. *Journal of Polymer Science, 2016*. doi: 10.1155/2016/7697031

71. Tønnesen, H. H., & Karlsen, J. (2002). Alginate in drug delivery systems. *Drug Development and Industrial Pharmacy, 28*(6), 621-30. doi: 10.1081/ddc-120003853

72. Abasalizadeh, F., Moghaddam, S.V., Alizadeh, E., Akbari, E., Kashani, E., Fazljou, S. M. B., Torbati, M., & Akbarzadeh, A. (2020). Alginate-based hydrogels as drug delivery vehicles in cancer treatment and their applications in wound dressing and 3D bioprinting. *Journal of Biological Engineering, 14*(8). doi: 10.1186/s13036-020-0227-7

73. Silva, E. A. & Mooney, D. J. (2007). Spatiotemporal control of vascular endothelial growth factor delivery from injectable hydrogels enhances angiogenesis. *Journal of Thrombosis and Haemostasis, 5*(3), 590-8. doi: 10.1111/j.1538-7836.2007.02386.x

74. Fenn, S. L., Miao, T., Scherrer, R. M., & Oldinski, R. A. (2016). Dual-Cross-Linked Methacrylated Alginate Sub-Microspheres for Intracellular Chemotherapeutic Delivery. *ACS applied materials & interfaces, 8*(28), 17775–83. doi: 10.1021/acsami.6b03245

75. Yigit, S., Sanyal, R., & Sanyal, A. (2011). Fabrication and functionalization of hydrogels through "click" chemistry. *Chemistry: An Asian Journal, 6*(10), 2648-59. doi: 10.1002/asia.201100440

76. Desai, R. M., Koshy, S. T., Hilderbrand, S. A., Mooney, D. J., & Joshi N. S. (2015). Versatile click alginate hydrogels crosslinked via tetrazine-norbornene chemistry. *Biomaterials, 50*, 30-37. doi: 10.1016/j.biomaterials.2015.01.048

77. Gao, L., Sun, Q., Wang, Y., Zhu, W., Li, X. X., Luo, Q., Li, X., & Shen, Z. (2017). Injectable poly(ethylene glycol) hydrogels for sustained doxorubicin release. *Polymers for Advanced Technologies, 28*(1), 35-40. doi: 10.1002/pat.3852

78. Mejia Oneto, J. M., Khan, I., Seebald, L., & Royzen, M. (2016). In vivo bioorthogonal chemistry enables local hydrogel and systemic pro-drug to treat soft tissue sarcoma. *ACS Central Science, 2*, 476-482. doi: 10.1021/acscentsci.6b00150

79. Agard, N. J., Prescher, J. A., & Bertozzi, C. R. (2004). A Strain-Promoted [3 + 2] Azide−Alkyne Cycloaddition for Covalent Modification of Biomolecules in Living Systems. *Journal of the American Chemical Society, 126*(46), 15046–47. doi: 10.1021/ja044996f

80. Brudno, Y., Desai, R. M., Kwee, B. J., Joshi, N. S., Aizenberg, M., & Mooney, D. J. (2015). In Vivo Targeting through Click Chemistry. *ChemMedChem, 10*(4), 617-620. doi:10.1002/cmdc.201402527

81. Moody, C. T., Palvai, S., & Brudno, Y. (2020). Click cross-linking improves retention and targeting of refillable alginate depots. *Acta Biomaterials, 112*, 112-121. doi: 10.1016/j.actbio.2020.05.033

82. Bouhadir, K. H., Alsberg, E., Mooney, D. J. (2001). Hydrogels for combination delivery of antineoplastic agents. Biomaterials, 22, 2625–2633. doi: 10.1016/s0142-9612(01)00003-5

83. Chewchuk, S., Boorman, T., Edwardson, D., & Parissenti, A. M. (2018). Bile Acids Increase Doxorubicin Sensitivity in ABCC1-expressing Tumour Cells. Scientific reports, 8(1), 5413. https://doi.org/10.1038/s41598-018-23496-y

84. Arteaga, C. L., & Engelman, J. A. (2014). ERBB receptors: from oncogene discovery to basic science to mechanism-based cancer therapeutics. Cancer cell, 25(3), 282–303. https://doi.org/10.1016/j.ccr.2014.02.025

85. Mishra, R., Hanker, A. B., & Garrett, J. T. (2017). Genomic alterations of ERBB receptors in cancer: clinical implications. Oncotarget, 8(69), 114371–114392. https://doi.org/10.18632/oncotarget.22825

86. Drake, J. M., Lee, J. K., & Witte, O. N. (2014). Clinical targeting of mutated and wild-type protein tyrosine kinases in cancer. Molecular and cellular biology, 34(10), 1722–1732. https://doi.org/10.1128/MCB.01592-13

87. Saleh, A. M., Wilding, K. M., Calve, S., Bundy, B. C., & Kinzer-Ursem, T. L. (2019). Non-canonical amino acid labeling in proteomics and biotechnology. *Journal of Biological Engineering*, *13*, 43. doi: 10.1186/s13036-019-0166-3

Chapter 2: Synthesis and Analysis of the EGFR-inhibitor Erlotinib Conjugated to an Aryl-Sulfone Linker

2.1 Introduction

EGFR inhibitors are used as chemotherapeutics against cancers that are positive for EGFR mutation or overexpression [1, 2]. This mutation and/or overexpression is a characteristic found in several cancer types, including approximately 48% of non-small cell lung cancers (NSCLCs) [3], 41% of pancreatic cancers [4], and 57% of glioblastomas [5]. By binding to EGFR, EGFR inhibitors prevent the protein from phosphorylating other cytoplasmic proteins that partake in cell signaling; more specifically, EGFR inhibitors prevent EGFR from initiating a transduction cascade that would otherwise result to cell proliferation, survival, migration, and focal adhesion [1, 6]. As such, EGFR inhibitors restrict the growth and spread of malignancies.

Erlotinib is a quinazoline-derived, highly selective EGFR inhibitor used to treat advanced or metastatic NSCLC and pancreatic cancer [1, 7]. It is an antagonist that reversibly competes with the ATP binding site located within EGFR; when erlotinib is bound, EGFR cannot autophosphorylate, and this terminates anti-apoptotic signaling pathways before they can be initiated [6, 8]. Erlotinib demonstrates remarkable efficacy in impeding the aggressiveness of NSCLCs and pancreatic cancer, as well as glioblastoma, though erlotinib has not been approved for treating glioma-type cancers [9-11]. Because of its efficacy, erlotinib is often used as a second-line monotherapy, especially for maintenance following treatment with a first line therapy but may be beneficial as a first-line monotherapy in some patients [11, 12].

Unfortunately, because EGFR is expressed ubiquitously, erlotinib has systemic side effects that limit its potential [13]. The EGFR-inhibiting effects are most apparent in the skin and

in the gastrointestinal tract, and side effects are common, typically including a skin rash, acne, pruritis, diarrhea, and anorexia. Rarer but more dangerous are side effects like renal failure, cardiac arrythmia, gastrointestinal perforations, and liver failure [13, 14]. Since these adverse effects are overwhelmingly the result of unnecessary systemic exposure, many of these effects could be prevented or dramatically minimized with localized delivery to a cancer site. Furthermore, because erlotinib is a substrate for P-glycoprotein and breast cancer resistance protein and these are both efflux pumps, it cannot persist within the central nervous system, limiting its potential for treating susceptible gliomas [7]. Because of this, erlotinib was selected as the chemotherapeutic of choice for demonstrating proof-of-concept for the hydrogel delivery system that is the focus of this dissertation.

In creating a click chemistry-based alginate hydrogel for drug delivery, drugs must be able to participate in a click reaction to bind to the gel and release active drug in a controlled, sustained fashion. To accomplish this, a prodrug version of the active drug must be created through conjugation to a linker. This linker should ideally be biocompatible, tunable, contain a click motif, and be relatively slow cleaving as to provide sustained therapeutic doses of drug over a sufficient period of time. Discussed in this chapter is the synthesis and characterization of a hydrolysable erlotinib prodrug containing a click motif.

2.2 Materials and Methods

Sodium phosphate dibasic anhydrous (Na2HPO4), potassium phosphate monobasic (KH2PO4), trifluoroacetic acid (TFA), HPLC-grade water, and HPLC-grade methanol were all

purchased from Fisher Scientific. Hydrochloric acid (HCl), dichloromethane (DCM) and n-methyl-2-pyrrolidone (NMP) were purchased from VWR. Sodium hydroxide (NaOH), dimethyl sulfoxide (DMSO) and methanol were purchased from Sigma Aldrich.

2.2.1 Synthesis of the Erlotinib Prodrug

Erlotinib prodrug was synthesized by a collaborator in the Pierce lab (North Carolina State University, Department of Chemistry). Briefly, the linker was formed by first adding sodium azide to a sealed tube containing 6-bromo-1-hexanol in anhydrous DMF. The reaction was resealed and heated to 110 for 8 hours. The resulting aqueous layer was extracted, and the organic layers were washed to remove residual DMF. The organic layers were then filtered over sodium sulfate and concentrated to form 6-azidohexan-1-ol as an oil. Separately, oxalyl chloride was added to a flask containing anhydrous DCM under nitrogen pressure, then cooled to -78^{o}C. DMSO was added to form an intermediate, after which 6-azidohexan-1-ol was added. The reaction was warmed to room temperature and stirred, then quenched with DI water. The aqueous layer was extracted with DCM, and the organic layers were filtered over sodium sulfate. The resulting crude oil was purified with flash chromatography, forming the resulting product, 6-azidohexanal. A solution of methyl phenyl sulfone in THF was added to lithium diisopropylamine, followed by the addition of aldehyde in THF, then 6-azidohexanal. The reaction was cooled and stirred for 2 hours, after which it was quenched with NH4Cl aqueous solution. The crude reaction was extracted with ethyl acetate, and the resulting organic layers were filtered over sodium sulfate and concentrated. The crude isolate was purified with flash chromatography, yielding the linker compound, 7-azido-1-(phenylsulfonul)heptan-2-ol.

For conjugating the linker, erlotinib in DCM solution was first modified through the addition of pyridine followed by triphosgene (BTC). The reaction was quenched with saturated

NH4Cl in aqueous solution and extracted with DCM. The organic layers were filtered over sodium sulfate, and the crude isolate was purified with flash chromatography to yield chloroformate erlotinib, or (6,7-bis(2-methoxyethoxy)quinazolin-4-yl)(3-ethynylphenyl)carbamic chloride. LiHMDS was added to the linker in anhydrous THF. Separately, chloroformate erlotinib was added to THF and cooled to -78^{o}C under nitrogen atmosphere. The alkoxide generated from the linker was added dropwise to the stirring solution of chloroformate erlotinib. The reaction was quenched with DI water after 4 hours and extracted with ethyl acetate. Organic layers were dried over sodium sulfate and concentrated, after which crude residue was dissolved in DCM and concentrated on a silica gel to be eluted via flash chromatography with an ethyl acetate/hexane gradient. This yielded the 7-azido-1-(phenylsulfonyl)heptan-2-yl (6,7-bis(2-methoxyethoxy)quinazolin-4-yl)(3-ethynylphenyl)carbamate conjugate herein known as “erlotinib prodrug.”

2.2.2 Compound Preparation and Storage

Erlotinib hydrochloride, the form of erlotinib that is orally administered, was provided by the Pierce lab (North Carolina State University, Department of Chemistry). Both erlotinib hydrochloride and erlotinib prodrug were separately dissolved in pure NMP to form stocks of various concentrations. Stocks were stored at -20^{o}C.

2.2.3 HPLC Analysis

An Agilent 1290 analytical HPLC and its accompanying software were used. The solvent system utilized HPLC-grade water and HPLC-grade methanol, both with 0.1% TFA. The column used was an Agilent C18 column (2.1 x 50 mm). The method was 8 minutes long and consisted of a mobile phase gradient of 10% MeOH in water that increased to 100% MeOH after 4

minutes. Methanol ran for 1 minute before returning to a gradient that ended with 10% MeOH in water after 3 minutes. Additionally, the column was heated to 40oC. The injection volume of samples was 5 µL and the flow rate was 0.5 mL/min. Absorbance of erlotinib was observed at 346 nm. Absorbance of erlotinib prodrug was observed at 336 nm.

2.2.4 Nanodrop Analysis

A Thermo Scientific Nanodrop 2000c with a 1 mm gap was used for nanodrop analysis. Absorbance of erlotinib was observed at 333 nm, and the absorbance of erlotinib prodrug was observed at 346 nm. A sample of erlotinib prodrug stock was diluted to a concentration of 100 µM. The absorbance was recorded 3 times and averaged. Beer's law was used to calculate the extinction coefficient using the average absorbance, the length of the light path (0.1 cm), and the concentration (0.0001 M).

2.2.5 Prodrug Kinetics Experiment

Phosphate buffer was prepared by dissolving Na2HPO4 and KH2PO4 in DI water to a concentration of 10 mM. The pH of the buffer was evaluated using a FiveEasy Standard pH Meter from Mettler Toledo and adjusted to 7.4 using 0.1 M HCl or 0.1 M NaOH. Solutions of erlotinib or erlotinib prodrug were prepared from stocks and consisted of a 1:4 ratio of NMP to phosphate buffer (10 mM, pH 7.4). The final concentration of each drug in solution was 200 uM. The solutions (n=2) were secured to a LabQuake Rotisserie Tube Rotator (Barnstead International) and incubated at 37 degrees with rotation. The solutions were sampled at hours 0, 2, 5, 12, 24, 48, 100, 196, 336, and 720 and run on analytical HPLC. The area under the curve (AUC) was measured for each peak at 346 nm ("free" erlotinib) and 336 nm (prodrug) at each time point.

2.3 Results

2.3.1 Synthesis and Structural Confirmation of the Erlotinib Prodrug

To create a prodrug-version of erlotinib, a linker containing a click motif was synthesized and conjugated to standard erlotinib (Figure 2.1). Conversion of 6-bromo-1-hexanol (S1) produced 6-azidohexan-1-ol (S2) in a clear oil with a yield of 80%. Synthesizing 6-azidohexanal (S3) from S2 yielded 94% of the starting mass and was also a clear oil. The linker, 7-azido-1-(phenylsulfonyl)heptan-2-ol (S4), was synthesized from S3 and yielded 56% of the starting mass.

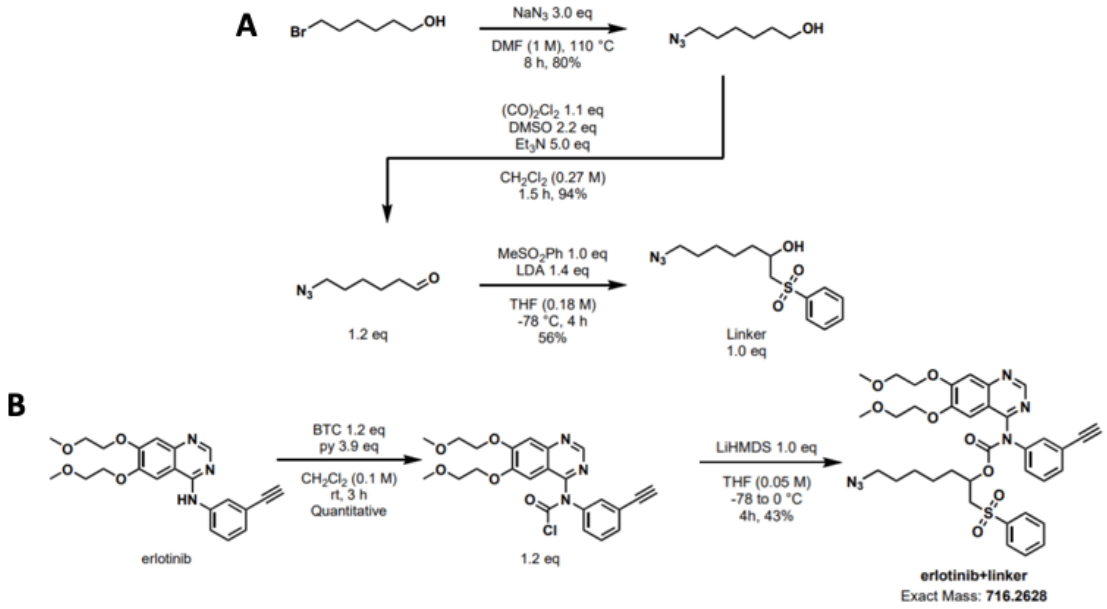

Figure 2.1. Schematic for the erlotinib prodrug synthesis reaction.

Standard erlotinib (S5), or (6,7-bis(2-methoxyethoxy)quinazolin-4-yl)(3-ethynylphenyl)amine, was transformed to (6,7-bis(2-methoxyethoxy)quinazolin-4-yl)(3-ethynylphenyl)carbamic chloride (S6), which was observed to be a pale, white oil with a

quantitative yield. This oil (1.2 eq.) was reacted with the linker, S4 (1 eq.), to ultimately produce 7-azido-1-(phenylsulfonyl)heptan-2-yl (6,7-bis(2-methoxyethoxy)quinazolin-4-yl)(3-ethynylphenyl)carbamate, or the desired erlotinib prodrug, as a white amorphous solid in a 42.49% yield. The structure of this erlotinib prodrug was confirmed with proton nuclear magnetic resonance (NMR) (Figure 2.2.) and carbon-13 NMR (Figure 2.3). Structural analysis with ChemDraw software predicted a mass of 716.26 g/mol (Figure 2.4). High resolution mass spectrometry revealed the exact mass to be 717.26967 g/mol.

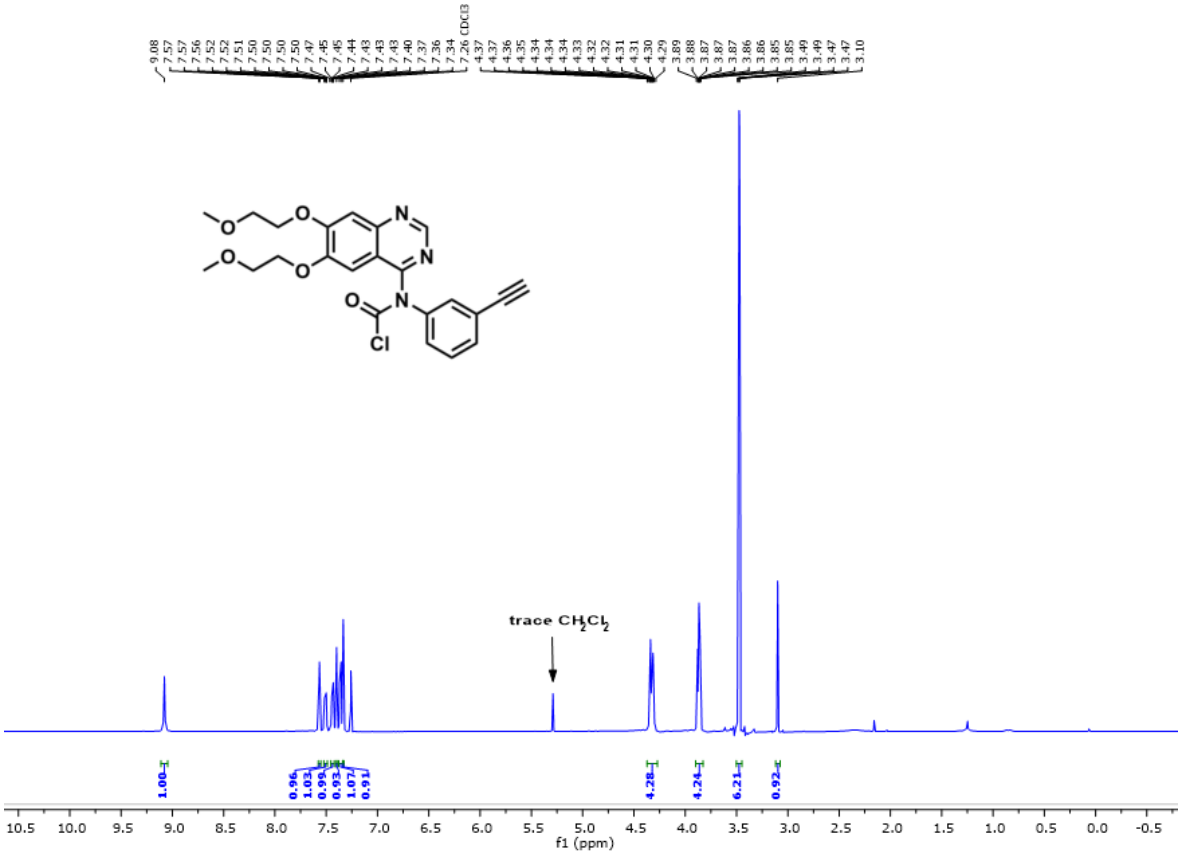

Figure 2.2. Proton nuclear magnetic resonance spectrograph confirming erlotinib prodrug structure.

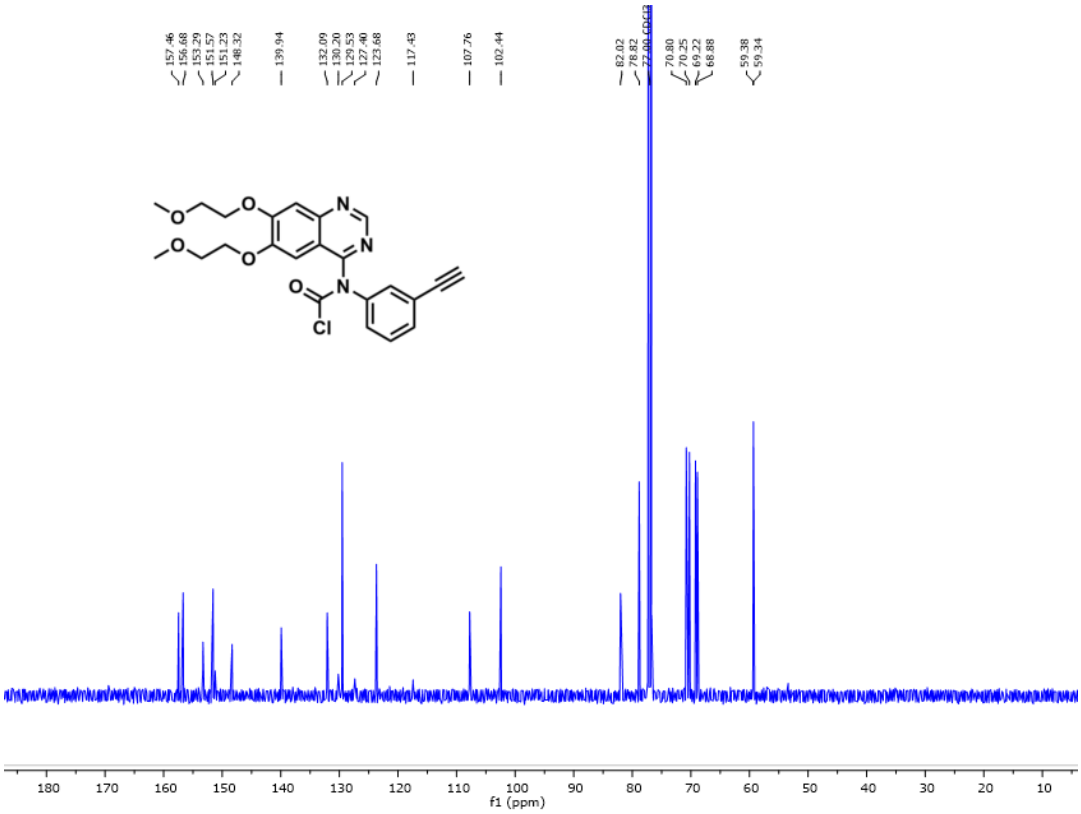

Figure 2.3. Carbon-13 nuclear magnetic resonance spectrograph confirming erlotinib prodrug structure.

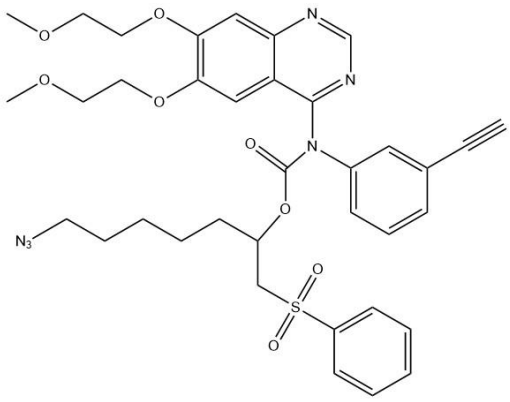

7-azido-1-(phenylsulfonyl)heptan-2-yl (6,7-bis(2-methoxyethoxy)quinazolin-4-yl)(3-ethynylphenyl)carbamate
Chemical Formula: $C_{36}H_{40}N_6O_8S$
Exact Mass: 716.26
Molecular Weight: 716.81
CLogP: 6.12792
LogS: -8.233

Figure 2.4. The structure of the erlotinib prodrug as analyzed by ChemDraw.

2.3.2 Baseline Analysis of the Erlotinib Prodrug with HPLC

Both erlotinib and erlotinib prodrug dissolved in a solution containing 20% NMP, 80% phosphate buffer showed distinct peaks when analyzed by HPLC. Standard erlotinib demonstrated an average retention time of 3.3 minutes (Figure 2.5), whereas the erlotinib prodrug had an average retention time of 4.4 minutes (Figure 2.6). 3D spectra of standard erlotinib revealed maximum absorbance of 346 nm, while 3D spectra of erlotinib prodrug revealed a maximum absorbance at 336 nm. Since these measurements were taken less than 1 hour after placing the drugs in aqueous solutions, the chromatograph for erlotinib prodrug demonstrates a small, barely detectable peak around 3.3 minutes.

Nanodrop analysis of 100 μM erlotinib prodrug yielded an average absorbance of 0.13233 when observed at 336 nm (Figure 2.7). Using Beer's law, the extinction coefficient was determined to be 1.3233×10^3.

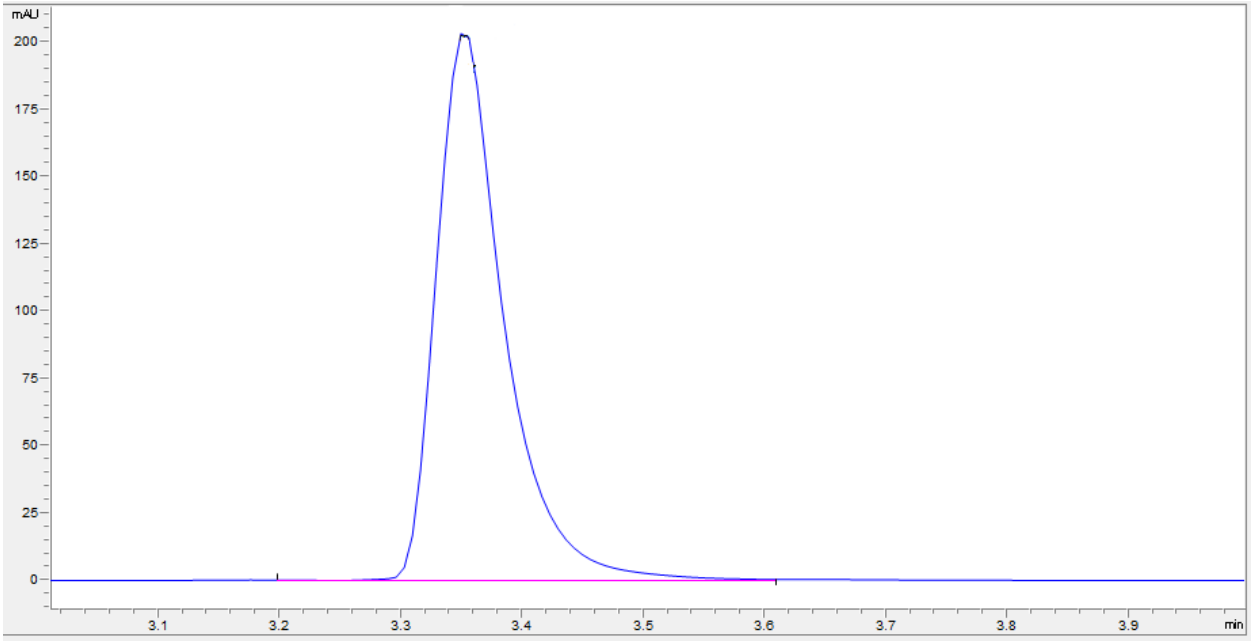

Figure 2.5. Chromatograph of standard erlotinib at its maximum absorbance of 346 nm.

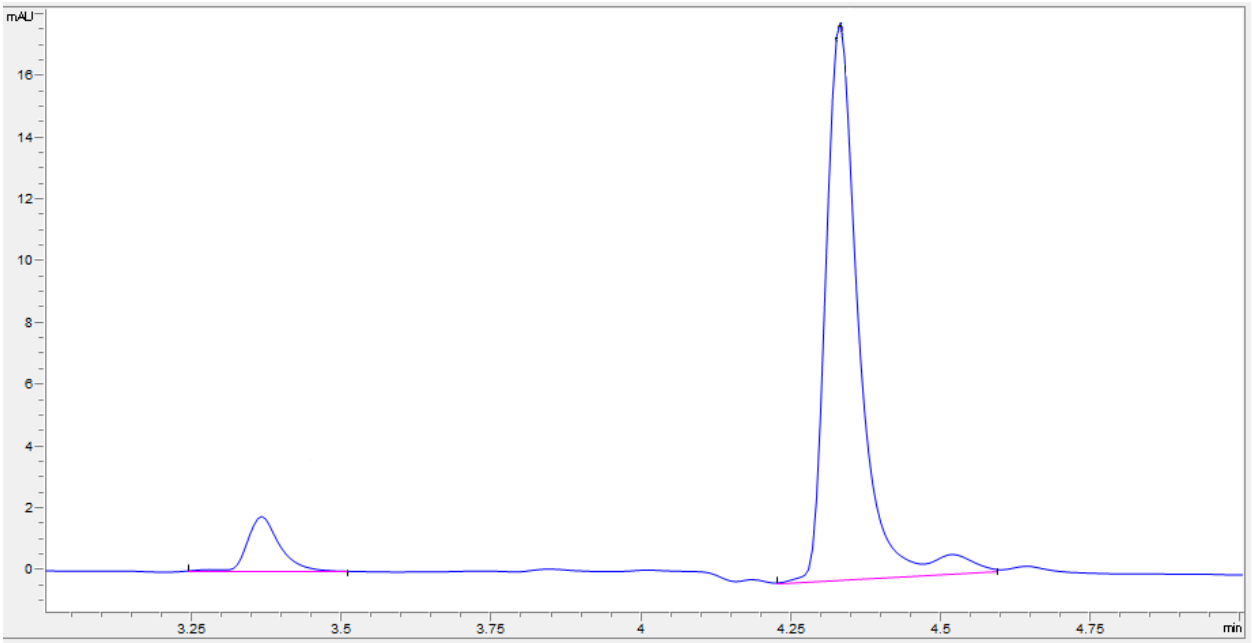

Figure 2.6. Chromatograph of erlotinib prodrug at standard erlotinib's maximum absorbance of 346 nm.

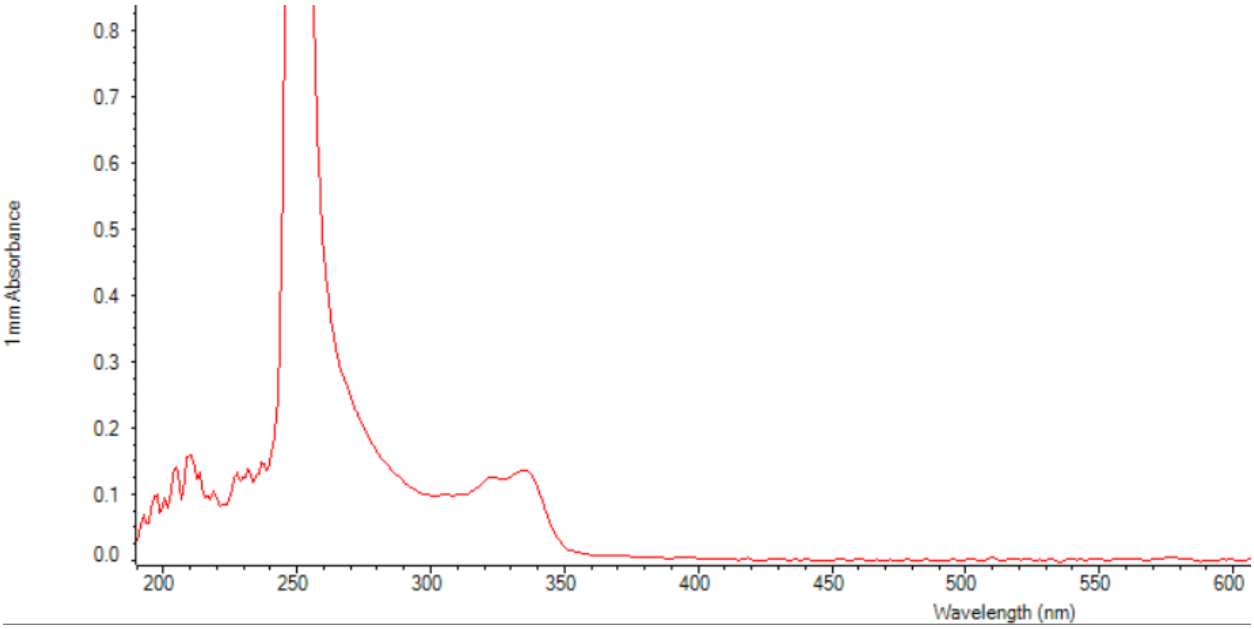

Figure 2.7. Nanodrop spectrograph of erlotinib prodrug.

2.3.3 Erlotinib Prodrug Kinetics

Erlotinib prodrug releases standard erlotinib through hydrolysis at the amide group that links the sulfone to erlotinib (Figure 2.8). The rate of linker hydrolysis was quantified by measuring the release of erlotinib from the prodrug over a period of 30 days. During that time, samples were incubated at 37 degrees with rotation. The rate of hydrolytic cleavage was determined to be 6.079×10^{-7} M/sec, and the half-life of the prodrug was found to be 80.454 hours (Figure 2.9). Consistent linker cleavage was observed with first-order kinetics, given the linearity of measured release on a semi-log plot (Figure 2.10).

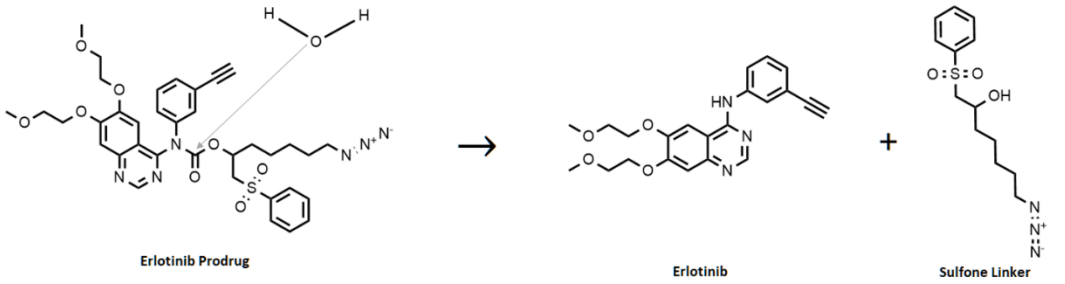

Figure 2.8. Schematic for the reaction of erlotinib release from the erlotinib prodrug by hydrolysis.

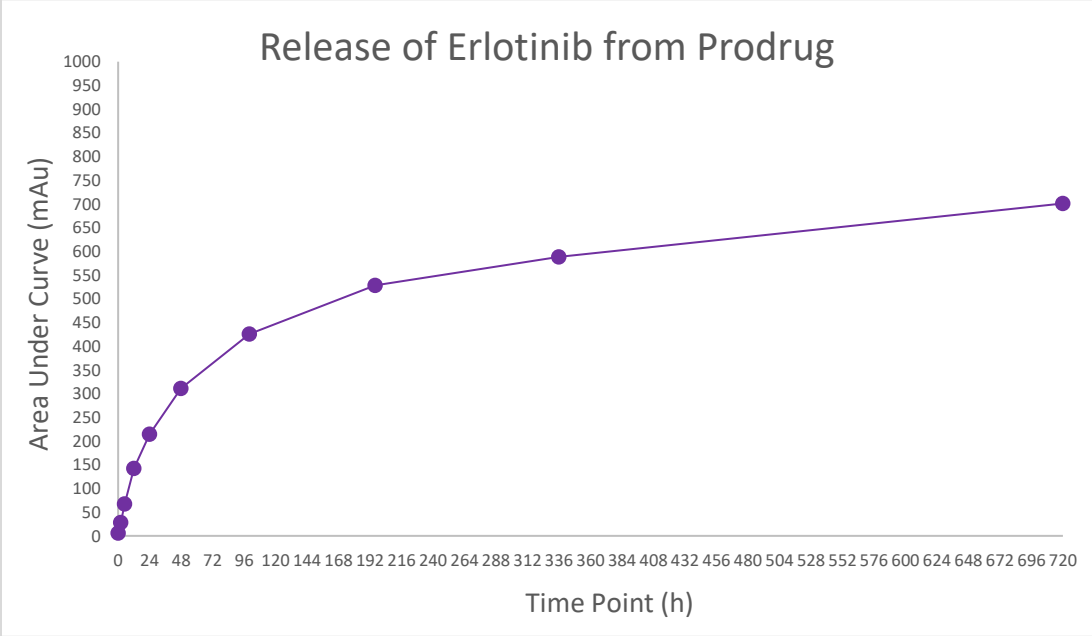

Figure 2.9. Release of erlotinib from erlotinib prodrug over time.

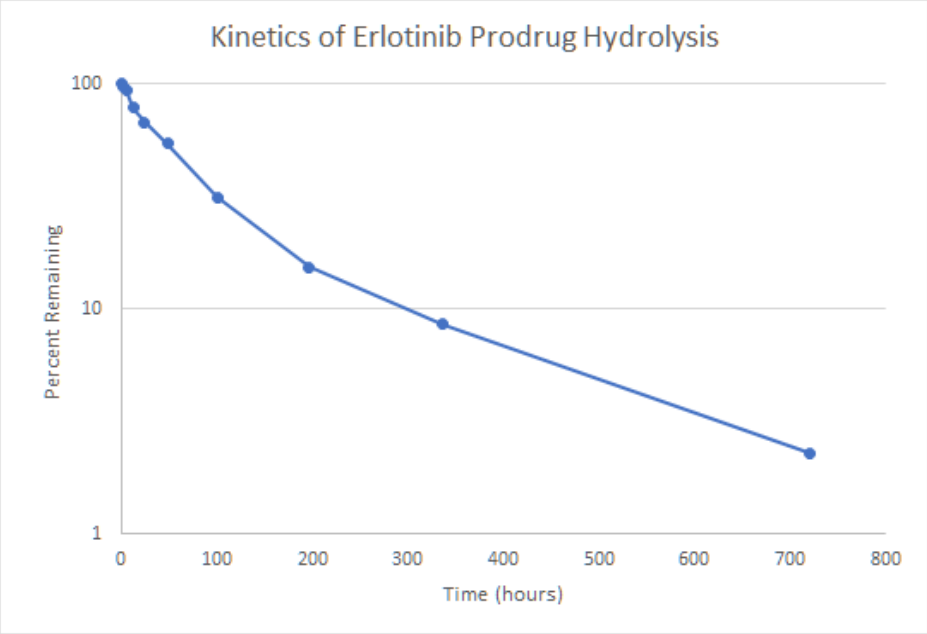

Figure 2.10. The kinetics of the erlotinib prodrug represented by a semi-log plot.

2.4 Discussion

Selecting the right linker molecule is important for developing a biocompatible drug delivery system that provides sustained release over a long period of time. For this purpose, a sulfone-based linker would be ideal. Sulfone linkers are commonly used in pharmaceutical manufacturing due to their safety, biological inertness, and tunability **[16].** To achieve a linker consistent with the proposed hydrogel system, a sulfone linker conjugated to an azide group that binds to a drug through its available alcohol group (Figure 2.1) was developed. In this case, erlotinib modified with an acyl chloride group readily reacts with the alcohol group on the linker to form erlotinib prodrug and hydrochloric acid as a by-product. Both ^{1}H NMR and ^{13}C NMR confirmed the structure of the erlotinib prodrug.

When the prodrug was received, it appeared to be a white, wax-like solid. The predictions made by ChemDraw include a predicted CLogP, or partition coefficient. As the Log P value of 6.12792 indicates, the prodrug proved to be highly hydrophobic and significantly more soluble in organic phases as opposed to aqueous phases. Originally, the prodrug was dissolved and stored in 100% DMSO; however, when attempting the kinetics experiments, chromatographs showed a continual loss of signal after 72 hours. It was theorized that the prodrug may be "crashing out" of solution; in response, a different solvent, NMP, was tried and proved to be successful in keeping erlotinib prodrug in solution over 30 days, at least up to a concentration of 200 μM. Higher concentrations were not tested. It was discovered, however, that prodrug is soluble in pure NMP up to a concentration of 50 mM.

When analyzed using HPLC, standard erlotinib was found to have a retention time of, on average, 3.3 minutes. The AUC calculated from standard erlotinib peaks remained consistent over the test period. The erlotinib prodrug had a retention time of 4.4 minutes, eluting after the mobile phase gradient had shifted to 100% methanol with 0.1% TFA. Erlotinib released from the prodrug, however, had a retention time consistent with standard erlotinib: 3.3 minutes. When analyzed at the zero-hour timepoint, the chromatograph for the erlotinib prodrug displayed a barely detectable peak around 3.3 minutes. This is likely erlotinib that has been released from the erlotinib prodrug. While the samples were run immediately after creating the solutions, a small amount of time passed before the samples were read on the HPLC due to the first sample being a blank. Hydrolytic cleavage of the erlotinib prodrug was found to have a rate of 6.079×10^{-7} M/sec, while the half-life was approximately 80.454 hours. Finally, nanodrop analysis revealed that the prodrug had an extinction coefficient of 1.3233×10^{3}. Considering all this, the erlotinib

prodrug appears to be an ideal candidate for a hydrogel drug delivery system given its sustained release over a period of 30 days.

2.5 References

1. Kim, M., Baek, M., & Kim, D. J. (2017). Protein Tyrosine Signaling and its Potential Therapeutic Implications in Carcinogenesis. *Current pharmaceutical design, 23*(29), 4226–4246. doi: 10.2174/1381612823666170616082125

2. Lim, W. A., & Pawson, T. (2010). Phosphotyrosine signaling: evolving a new cellular communication system. *Cell, 142*(5), 661–667. doi: 10.1016/j.cell.2010.08.023

3. Li, A. R., Chitale, D., Riely, G. J., Pao, W., Miller, V. A., Zakowski, M. F., Rusch, V., Kris, M. G., & Ladanyi, M. (2008). EGFR mutations in lung adenocarcinomas: clinical testing experience and relationship to EGFR gene copy number and immunohistochemical expression. *The Journal of molecular diagnostics : JMD, 10*(3), 242–248. doi: 10.2353/jmoldx.2008.070178

4. Oliveira-Cunha, M., Newman, W. G., & Siriwardena, A. K. (2011). Epidermal growth factor receptor in pancreatic cancer. *Cancers, 3*(2), 1513–1526. doi: 10.3390/cancers3021513

5. Brennan, C. W., Verhaak, R. G., McKenna, A., Campos, B., Noushmehr, H., Salama S. R., Zheng, S., Chakravarty, D., Sanborn, J.Z., Berman, S.H., et al. (2013). The somatic genomic landscape of glioblastoma. *Cell, 155*, 462–477. doi: 10.1016/j.cell.2013.09.034.

6. Guo, L., Kozlosky, C. J., Ericsson, L. H., Daniel, T. O., Cerretti, D. P., & Johnson, R.S. (2003). Studies of ligand-induced site-specific phosphorylation of epidermal growth factor receptor. *Journal of the American Society for Mass Spectrometry, 14,* 1022–1031. doi: 10.1016/S1044-0305(03)00206-X

7. Lan, M. Y., Hsu, Y. B., Lan, M. C., Chen, J. P., & Lu, Y. J. (2020). Polyethylene Glycol-Coated Graphene Oxide Loaded with Erlotinib as an Effective Therapeutic Agent for Treating Nasopharyngeal Cancer Cells. *International journal of nanomedicine*, *15*, 7569–7582. doi: 10.2147/IJN.S265437

8. Normanno, N., Maiello, M. R., & De Luca, A. (2003). Epidermal growth factor receptor tyrosine kinase inhibitors (EGFR-TKIs): simple drugs with a complex mechanism of action? *Journal of Cell Physiology, 194*(1), 13-9. doi: 10.1002/jcp.10194. PMID: 12447985.

9. Wang, Y., Hu, G. F., Zhang, Q. Q., Tang, N., Guo, J., Liu, L. Y., Han, X., Wang, X., & Wang, Z. H. (2016). Efficacy and safety of gemcitabine plus erlotinib for locally advanced or metastatic pancreatic cancer: a systematic review and meta-analysis. *Drug design, development and therapy*, *10*, 1961–1972. https://doi.org/10.2147/DDDT.S105442

10. Reddick, S. J., Campagne, O., Huang, J., Onar-Thomas, A., Broniscer, A., Gajjar, A., & Stewart, C. F. (2019). Pharmacokinetics and safety of erlotinib and its metabolite OSI-420 in infants and children with primary brain tumors. *Cancer chemotherapy and pharmacology*, *84*(4), 829–838. doi: 10.1007/s00280-019-03921-3

11. Bulbul, A., & Husain, H. (2018). First-Line Treatment in EGFR Mutant Non-Small Cell Lung Cancer: Is There a Best Option?. *Frontiers in oncology*, *8*, 94. doi: 10.3389/fonc.2018.00094

12. Lee, S. M., Khan, I., Upadhyay, S., Lewanski, C., Falk, S., Skailes, G., Marshall, E., Woll, P. J., Hatton, M., Lal, R., Jones, R., Toy, E., Chao, D., Middleton, G., Bulley, S.,

Ngai, Y., Rudd, R., Hackshaw, A., & Boshoff, C. (2012). First-line erlotinib in patients with advanced non-small-cell lung cancer unsuitable for chemotherapy (TOPICAL): a double-blind, placebo-controlled, phase 3 trial. *The Lancet. Oncology*, *13*(11), 1161–1170. doi: 10.1016/S1470-2045(12)70412-6

13. Choi, H. D., & Chang, M. J. (2020). Eye, hepatobiliary, and renal disorders of erlotinib in patients with non-small-cell lung cancer: A meta-analysis. *PloS one*, *15*(7), e0234818. doi: 10.1371/journal.pone.0234818

14. Coudert, B., Ciuleanu, T., Park, K., Wu, Y. L., Giaccone, G., Brugger, W., Gopalakrishna, P., & Cappuzzo, F.; SATURN Investigators. (2012). Survival benefit with erlotinib maintenance therapy in patients with advanced non-small-cell lung cancer (NSCLC) according to response to first-line chemotherapy. *Annals of Oncology*, *23*(2), 388-94. doi: 10.1093/annonc/mdr125

15. M. J. Greenberg. (1980). The importance of hydrophobic properties of organic compounds on their taste intensities: a quantitative structure-taste-intensity study. J. Agirc. Food Chem., 28(3): 562–566.

16. Feng, M., Tang, B., Liang, S. H., & Jiang, X. (2016). Sulfur Containing Scaffolds in Drugs: Synthesis and Application in Medicinal Chemistry. *Current topics in medicinal chemistry*, *16*(11), 1200–1216. doi: 10.2174/1568026615666150915111741

Chapter 3: Synthesis and Analysis of an Alginate Hydrogel containing the Erlotinib-Linker Conjugate

3.1 Introduction

Alginate-based hydrogels utilizing click chemistry have shown promise in drug delivery. The SPAAC reaction in particular has been shown to be beneficial in vitro and in vivo due to its high specificity and biological inertness [1]. Utilizing the SPAAC reaction to covalently crosslink alginate hydrogels results in a more stable gel that produces a reduced immune response and is well-retained in tissues [2]. Additionally, the SPAAC reaction can be used to load drugs or prodrugs containing available azide groups into a hydrogel [3].

Recently, it was shown that tBCN successfully crosslinks modified alginate hydrogels and improves the hydrogel's stability, non-immunogenicity, and tissue retention [2]. TBCN is a four-armed compound containing a cyclooctyne group on each arm. These groups can bind azide-modified alginate strands through SPAAC reactions, leading to the formation of a hydrogel. If there are "arms" available on the tBCN molecule, then the molecule can participate in additional SPAAC reactions with an azide-containing molecule.

In this chapter, the synthesis of tBCN-crosslinked hydrogels and the utility of these gels as drug delivery vehicles will be explored. The erlotinib prodrug contains an available azide that can bind to the cyclooctyne groups on tBCN. On the condition that tBCN still has some of the groups available after the addition of the prodrug, then the tBCN could still successfully crosslink azide-modified alginate to form a hydrogel. The resulting hydrogel would then release free erlotinib in a sustained fashion at the rate of linker hydrolysis. This will provide proof-of-

concept for the proposed click chemistry-based alginate hydrogel drug delivery system that is the focus of this dissertation.

3.2 Methods and Materials

Sodium phosphate dibasic anhydrous (Na2HPO4), potassium phosphate monobasic (KH2PO4), trifluoroacetic acid (TFA), HPLC-grade water, HPLC-grade methanol, LLC-Cell counting kit-8 (CCK-8), and penicillin-streptomycin were all purchased from Fisher Scientific. Hydrochloric acid (HCl), dichloromethane (DCM) and n-methyl-2-pyrrolidone (NMP) were purchased from VWR. Sodium hydroxide (NaOH), dimethyl sulfoxide (DMSO), poly(amidoamine) (PAMAM), triethylamine, calcium sulfate, calcium chloride, and methanol were purchased from Sigma Aldrich. Ultrapure alginate (Pronova UP MVG-sodium alginate, MW = 250 kDa, 67% guluronic acid) was purchased through NovaMatrix. Fetal bovine serum was purchased from the tissue culture facility at the University of North Carolina, Chapel Hill, and the supplier is VWR. Trypsin (0.05% EDTA) and Dulbecco's Modified Eagle Medium (DMEM) was purchased from Gibco.

3.2.1 Cell Culture

The A431 cell line was obtained through the tissue culture facility at the University of North Carolina, Chapel Hill. The received vial had a recorded freeze date of September 20, 2017, and was on passage 19. It was originally supplied by ATCC (CRL-1555). The frozen stock of cells was initiated into a T-75 culture flask with pre-warmed media (DMEM, 10% FBS, 1% penicillin-streptomycin). Media was changed every two to three days, and the cells were passaged at approximately 70% confluency two to three times per week for maintenance. To

passage for maintenance, cells were digested with trypsin (0.05% EDTA) and split 1:5 into new T-75 vessels.

3.2.2 Cytotoxicity Experiment

To assess the cytotoxicity of NMP on A431 cells, NMP was added to DMEM to a concentration of 2% in a 96-well plate. A 1:2 serial dilution was performed until a concentration of 0.0625% was reached (5 dilutions total). Once the serial dilution was complete, an equal volume of A431 cell suspension was added to the wells such that the wells contained 5,000 cells/well. The addition of cell suspension diluted the NMP in media to a concentration range of 0.03125 – 1%. Cells were incubated for 48 hours (37^{o}C, 5% CO_2). A CCK-8 assay was performed by aspirating the old media out of the wells and replacing it with DMEM containing 10% CCK-8. The cells were then incubated for 2 hours, the plate was read on a Tecan GENios microplate reader, and the results were analyzed using the microplate reader's accompanying software.

To assess the cytotoxicity of erlotinib prodrug on A431 cells, a stock of erlotinib or erlotinib prodrug was diluted in DMEM media to a concentration of 160 µM. A 1:4 serial dilution was performed until a concentration of 0.001221 µM was reached (9 dilutions total). NMP concentration was kept consistent at 0.4% of the total volume. Once the serial dilution was complete, an equal volume of A431 cell suspension was added to the wells such that the wells contained 5,000 cells/well. The addition of cell suspension resulted in a drug concentration range of 0.000305 – 80 µM and a consistent concentration of NMP at 0.2%. Cells were incubated for 48 hours (37^{o}C, 5% CO_2). A CCK-8 assay was performed as described above.

3.2.3 Synthesis of t-BCN

To synthesize t-BCN, a solution of BCN was first created by dissolving 25 mg of BCN-NHS in 400 µL of DMSO, then adding 400 µL of methanol. Once the BCN-NHS was fully dissolved, 14.2 µL of triethlamine was added to the solution, followed by 52.8 µL of PAMAM. The solution was vortexed and left to sit for approximately 10 minutes. The BCN solution was purified using Agilent 1100 series preparatory HPLC and a XBridge Prep C18 OBD column (5 µM, 30 x 150 mm). The 20-minute method consisted of a gradient beginning with 100% water with 0.1% TFA and transitioning to 100% methanol with 0.1% TFA over the course of 12 minutes. The flow rate was 20 mL/min, and the fractions collected were based on detection of a peak with a retention time of 11 minutes. Fractions associated with the t-BCN peak (210 nm) were collected and placed on a rotary evaporator for approximately 15 minutes to evaporate the methanol. The remaining solution was washed with methanol and transferred to a new vial before being placed on the rotary evaporator again. Once the methanol was again removed, the vial containing the t-BCN solution was frozen in a -20^{o}C freezer overnight. The frozen solution was freeze-dried on a lyophilizer for 2 days. The resulting solid compound was weighed, dissolved in NMP to a concentration of 10 mM, and stored at -20^{o}C.

3.2.4 Synthesis of t-BCN Crosslinked Alginate Hydrogels

For the modifying alginate to contain azide groups, 1 gram (4 µmol; 1 eq.) of medical grade, high molecular weight alginate with high guluronic acid content (NovaMatrix) was dissolved in an 100 mM MES buffer (200 mL, pH 6.5) overnight. Azide-PEG4-amine (Lumiprobe-1868, 8 mmol; 2,000 eq.) was added and the solution stirred at room temperature. Following that, 1-ethyl-3-[3-dimethylaminopropyl]carbodiimide hydrochloride (EDC, 2 mmol; 500 eq.) and sulfo-N-hydroxysuccinimide (sNHS, 1 mmol; 250 eq.) were mixed together and

split into three doses which were given every eight hours. The solution stirred for an additional eight hours following the final dose. The solution underwent dialysis using 4 L of water changed 2-3 per day with decreasing NaCl content. Finally, the solutions were frozen at -20^{o}C overnight and freeze-dried using a lyophilizer. This produced "low-azide alginate." Low-azide alginate was dissolved in phosphate buffer (10 mM, pH 7.4) at a concentration of 20 mg alginate per 1 mL of buffer. This solution was stirred on a stir plate overnight to ensure full dissolution of alginate.

A solution was created using T-BCN stock (10 mM, 60 µL), 15 µL of 50 mM prodrug stock (or NMP for controls), and 15 µL $CaSO_4$ and vortexed. This mixture transferred to a 1 mL syringe. A total of 900 µL of alginate solution was transferred to a 3 mL syringe, which was then connected to the 1 mL syringe via a Luer lock coupler. The plungers of the syringes were alternatively pressed approximately 20 times to mix the solutions. Once mixed, 300 µL of the final solution was injected into microcentrifuge tubes and allowed to gel at room temperature for 24 hours. The hydrogels were transferred into new tubes containing 600 µL of pre-warmed (37^{o}C) release buffer (20% NMP, 77% phosphate buffer, 3% $CaCl_2$). The concentration of prodrug in the final volume containing both gel and release buffer was 250 µM. The tubes were transferred to a shaking incubator (37^{o}C, 90 RPM) for incubation and sampled at 0, 24, 36, 72, and 120 hours.

3.2.5 HPLC Analysis

An Agilent 1290 analytical HPLC and its accompanying software were used. The solvent system utilized HPLC-grade water and HPLC-grade methanol, both with 0.1% TFA. The column used was an Agilent C18 column (2.1 x 50 mm). The method was 8 minutes long and consisted of a mobile phase gradient of 10% MeOH in water that increased to 100% MeOH after 4 minutes. Methanol ran for 1 minute before returning to a gradient that ended with 10% MeOH in

water after 3 minutes. Additionally, the column was heated to 40^{o}C. The injection volume of samples was 5 µL, and the flow rate was 0.5 mL/min. Absorbance of erlotinib was observed at 346 nm with a retention time of 3.3 minutes. Absorbance of erlotinib prodrug was observed at 336 nm with a retention time of 4.4 minutes.

3.3 Results

3.3.1 Assessment of the Erlotinib Prodrug's Cytotoxicity

The A431 cell line is an epidermoid carcinoma cell line that has demonstrated overexpression of EGFR and sensitivity to EGFR inhibitors [4, 5]. Before the effects of the erlotinib prodrug could be assessed on A431s, the toxicity of the carrier solvent, NMP, needed to be evaluated. NMP is commonly used as a drug solubilizer, but its bioactivity is not well defined [6], making it crucial to determine its toxicity against cancer cells as to not misattribute cytotoxic effects to erlotinib prodrug erroneously. A serial dilution of NMP in A431s was completed with NMP concentrations ranging from 0.03125 – 1%. A CCK-8 assay performed after cells incubated with NMP for 48 hours showed that concentrations of NMP of 0.5% and higher were highly cytotoxic to A431s relative to the control group (Figure 3.1). The EC_{50} of NMP for A431s was determined to be 0.32%.

To evaluate the cytotoxic effects of the erlotinib prodrug against A431s, a 1:4 serial dilution was performed, giving a concentration range of 0.0003 – 80 µM (Figure 3.2). A431s demonstrated a higher tolerance for erlotinib prodrug over 48 hours compared to standard erlotinib (Figure 3.3), implying that the erlotinib prodrug produces less of an effect than standard erlotinib does over the course of 48 hours.

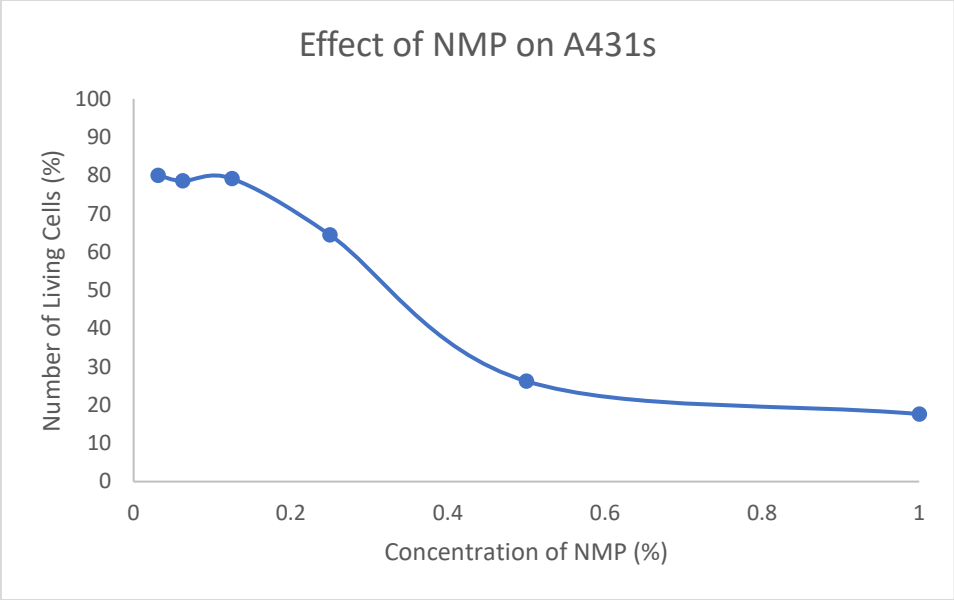

Figure 3.1. The effect of NMP concentration on A431s after 48 hours of incubation. The EC_{50} was determined to be 0.32% NMP for this cell line.

	1	2	3	4	5	6	7	8	9	10	11	12
A	Conc. (µM)	80	20	5	1.25	0.3125	0.0781	0.0195	0.0049	0.0012	0.0003	
B												
C												
D												
E												
F		Cells + NMP			Cells Only				Media Only			
G												
H												

Figure 3.2. The schematic for the 96-well plate used for assessing the cytotoxicity of the erlotinib prodrug. "Cells + NMP" refers to cells incubated with 0.2% NMP in media, "cells only" refers to cells incubated in DMEM media alone, and "media only" refers to wells containing only media and no cells.

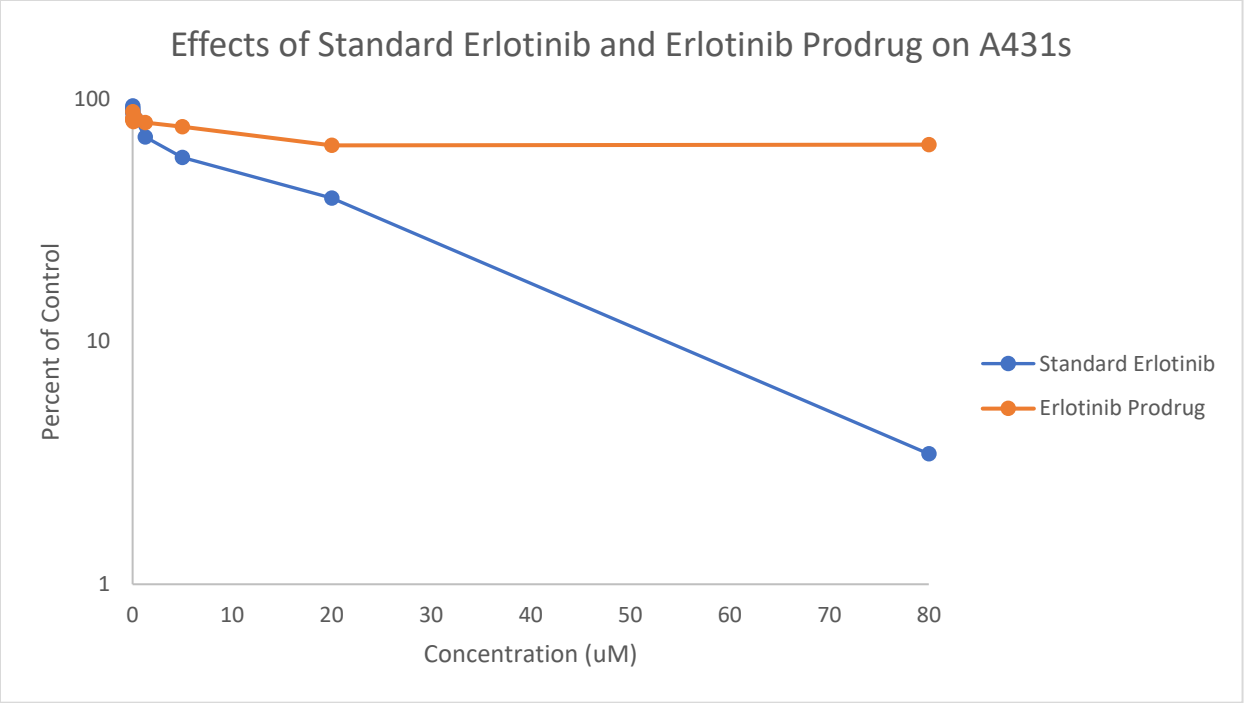

Figure 3.3. Graph representing the effects of standard erlotinib and the erlotinib prodrug after 48 hours as determined by a CCK-8 assay.

3.3.2 Synthesis and Purification of t-BCN

T-BCN was successfully synthesized through mixing triethylamine and PAMAM with BCN-NHS in solution (Figure 3.4, Table 3.1). Preparatory HPLC yielded 3 collectable fractions (approximately 12 mL) which were combined and placed on a rotary evaporator. Removal of methanol resulted in the solution turning into a milky-white color. Freeze-drying of the solution yielded 14.4 mg of a white powder-like solid. This powder was dissolved in NMP to yield a concentration of 10 mM. Creation of a 20 mM stock was attempted, but t-BCN was not completely soluble at this concentration.

Table 3.1. PAMAM-amine and triethylamine react optimally with BCN-NHS in specific ratios, given as equivalents (eq.) in the table below. Mass (g), molecular weight (M.W.), moles, concentration, and volume are given for synthesizing approximately 1 mL of BCN solution.

	Mass (g)	***M.W.***	***Moles***	***Stock Conc. (g/L)***	***Stock volume (L)***	***Eq.***
BCN-NHS	2.50×10^{-2}	291.3	8.58×10^{-5}	N/A	N/A	4.2
Triethylamine	1.03×10^{-2}	101.2	1.02×10^{-4}	726	1.42×10^{-5}	5
PAMAM	1.06×10^{-2}	517	2.04×10^{-5}	200	5.28×10^{-5}	1

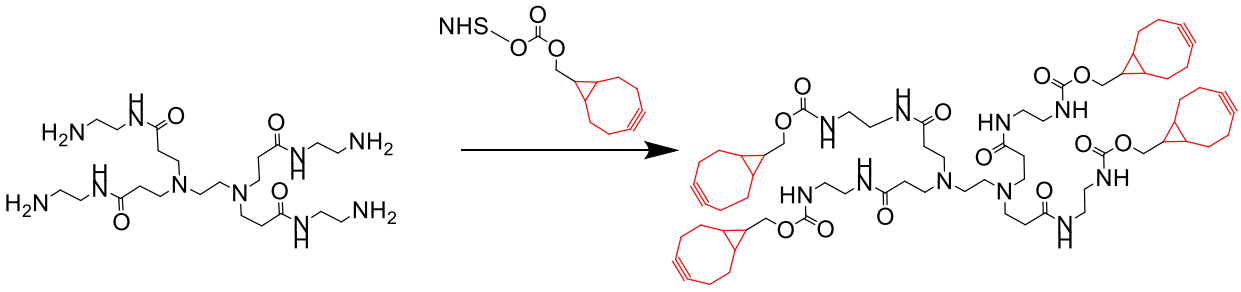

Figure 3.4. Reaction for synthesizing t-BCN. The four-armed PAMAM dendrimer reacts with BCN-NHS to yield a tetramer of BCN in a single step. T-BCN can then be purified by preparatory HPLC.

3.3.3 Synthesis of Prodrug-containing Hydrogels

Initial attempts at making a prodrug-containing t-BCN crosslinked hydrogel involved mixing prodrug in NMP, t-BCN in NMP, and low-azide alginate solution together through interlocked syringes before injecting the mixture into a microcentrifuge tube to gel at room temperature. Even after 48 hours, these mixtures did not undergo full gelation, instead producing a viscous liquid. To remedy this issue, a small amount of calcium sulfate was added to the mixture. This facilitated full gelation after 24 hours (Figure 3.5).

Figure 3.5. A picture of the t-BCN gels containing erlotinib prodrug and 24 hours of gelation.

After release buffer was added to the gels and the gels were incubated over five days, no disintegration of the gels was visually observed. HPLC analysis confirmed release of erlotinib from the gels (Figure 3.7). Interestingly, some prodrug appeared to be in the release buffer as well, though the peak was not well defined. No release of either erlotinib or prodrug was observed at any other time point (Figure 3.6).

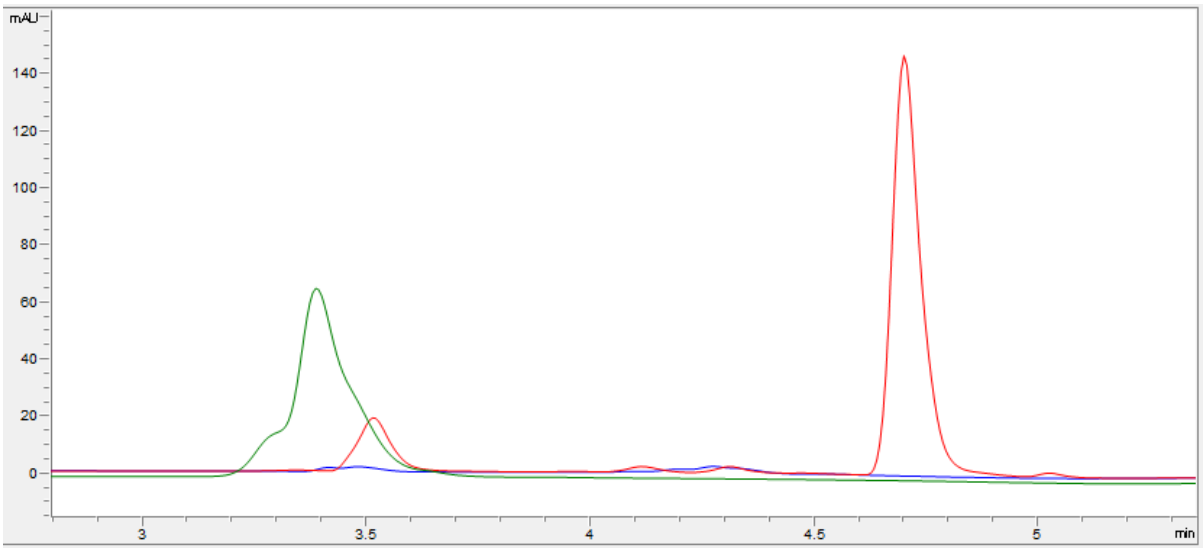

Figure 3.6. Chromatograph of erlotinib released from prodrug-containing t-BCN hydrogels at the 36-hour time point (346 nm). The green line indicates the standard erlotinib control, the red line indicates the prodrug control, and the blue line indicates the sampled release buffer from a prodrug-containing hydrogel.

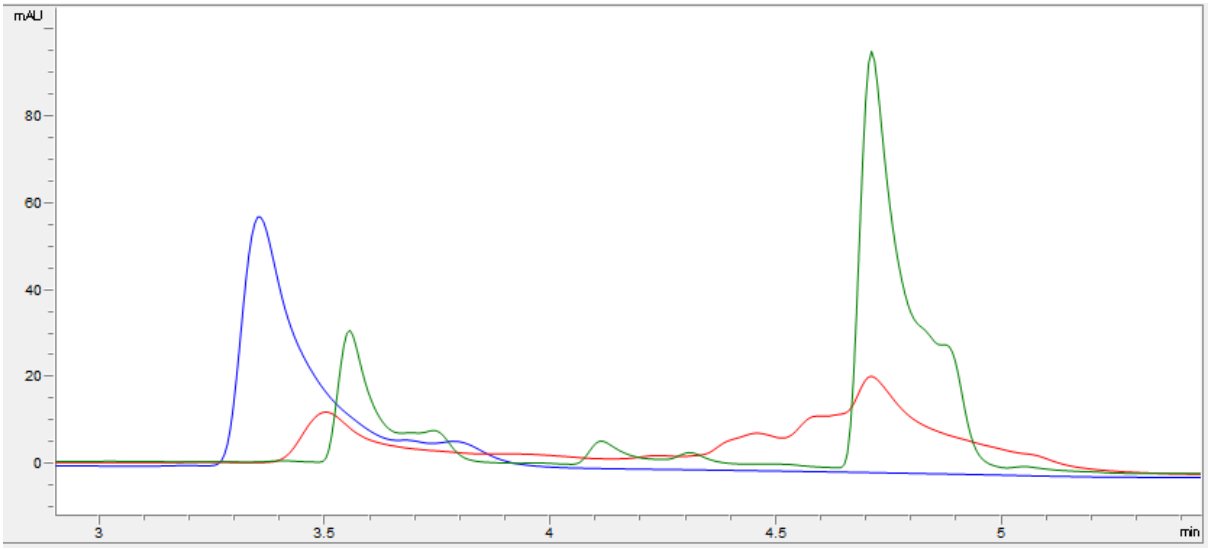

Figure 3.7. Chromatograph of erlotinib released from prodrug-containing t-BCN hydrogels at the five-day (120 hour) time point (346 nm). The blue line indicates the standard erlotinib control, the green line indicates the prodrug control, and the red line indicates the sampled release buffer from a prodrug-containing hydrogel.

3.4 Discussion

Before attempting to synthesize hydrogels that contained erlotinib prodrug, the toxicity and effectiveness of erlotinib prodrug was first evaluated through CCK-8 assay on a susceptible cell line, A431. As expected, A431s demonstrated inhibited growth in the presence of standard erlotinib. This inhibition of growth was not observed to the same extent in A431s treated with erlotinib prodrug. This may be due to the half-life of the prodrug, which is 80.454 hours. After only 48 hours of incubation, less than one-third of the prodrug had been hydrolyzed. This would result in low concentrations of erlotinib and a low level of inhibition of proliferation. Additionally, the lack of inhibition indicates nontoxicity of the erlotinib prodrug, indicating that the prodrug that has not been hydrolyzed is not directly harmful to cells.

T-BCN was successfully synthesized and was fully soluble in NMP up to a concentration of 10 mM. T-BCN appeared to crosslink the low-azide alginate to some extent, as the resulting solution was semi-viscous, though it was not a solid gel. This occurred in both the control and the prodrug-containing gels, so it is not likely to be a result of the interaction between t-BCN and prodrug. Additionally, using t-BCN in a solution of DMSO instead of NMP did not result in gelation either, therefore NMP is unlikely to be responsible for this effect. The lack of full gelation may be to the ratio of t-BCN to available azides in the low-azide alginate gel: without enough available azides, or alternatively not enough available t-BCN, crosslinking cannot occur efficiently. To remedy this, a small volume of calcium sulfate (100 mg/mL) was added to the mixture of t-BCN and prodrug. This resulted in successful gelation (Figure 3.6); one potential complication of this solution is that the gels may have decreasing integrity over time due to the calcium crosslinking. Ionic crosslinking of alginate hydrogels is not stable over prolonged periods of time as there is gradual release of divalent cations. Covalent crosslinking is far more

stable, so a more-ideal solution to the crosslinking issue encountered would be to find the minimum number of t-BCN-azide crosslinks needed to form a stable gel.

The synthesized hydrogels were placed in release buffer, incubated, and sampled at 0-, 24-, 48-, 72-, and 120-hours post-addition of the buffer. Since the hydrogel contains water, hydrolysis was likely occurring during the 24 hours of gelation. Of note, no other gelation times were tested, so the gels may have sufficient integrity before 24 hours. When release buffer was added, the gels swelled with additional water; whether or not the diffusion of released erlotinib may be affected by this influx was not determined. HPLC analysis of samples showed no presence of erlotinib or prodrug at 0-, 24-, 48-, or 72-hour time points (Figure 3.7); presence of both erlotinib and prodrug was detected at 120-hours (Figure 3.8). Of note, at 346 nm, the wavelength that standard erlotinib absorbed best at, more erlotinib prodrug was detected than released erlotinib. This is surprising, as erlotinib prodrug should be bound to the t-BCN rather than be unbound in the gel or the buffer. This may be due to a low number of t-BCN molecules, as this was also thought to be behind the issue with crosslinking azide-modified alginate strands. Additionally, the peaks observed in the chromatograph for release buffer sampled from prodrug-containing gels after 120 hours were undefined, wavy, and broad. This corresponded to abnormally high pressure during the HPLC run. It was thought that alginate strands may be present in the samples, leading to clogging of the HPLC column or filters and increased pressure in the system. The filters and columns were flushed, resulting in normal pressure, and the samples were re-run after being filtered with GVS Separa Syringeless 32 mm Filter Vials. These filters had a pore size of 0.2 µM, which is a pore sized used by another study that filtered alginate solutions [7], but this did resolve the issue with pressure in this case. Overall, it appears

that this hydrogel system shows promise in providing sustained release of erlotinib from erlotinib prodrug, though there needs to be optimization of the ratio of t-BCN to azides and prodrug.

3.5 References

1. Debets, M. F., van Berkel, S. S., Dommerholt, J., Dirks, A. T., Rutjes, F. P., & van Delft, F. L. (2011). Bioconjugation with strained alkenes and alkynes. *Accounts of Chemical Research, 44*(9), 805-15. doi: 10.1021/ar200059z

2. Moody, C. T., Palvai, S., & Brudno, Y. (2020). Click cross-linking improves retention and targeting of refillable alginate depots. *Acta Biomaterials, 112,* 112-121. doi: 10.1016/j.actbio.2020.05.033

3. DeForest, C., Polizzotti, B. & Anseth, K. (2009). Sequential click reactions for synthesizing and patterning three-dimensional cell microenvironments. *Nature Materials, 8,* 659–664 (2009). doi: 10.1038/nmat2473

4. Mincione, G., Di Marcantonio, M. C., Tarantelli, C., Savino, L., Ponti, D., Marchisio, M., Lanuti, P., Sancilio, S., Calogero, A., Di Pietro, R., & Muraro, R. (2016). Identification of the zinc finger 216 (ZNF216) in human carcinoma cells: a potential regulator of EGFR activity. *Oncotarget*, *7*(46), 74947–74965. doi: 10.18632/oncotarget.12509

5. Modjtahedi, H., Cho, B. C., Michel, M. C., & Solca, F. (2014). A comprehensive review of the preclinical efficacy profile of the ErbB family blocker afatinib in cancer. *Naunyn-Schmiedeberg's archives of pharmacology, 387*(6), 505–521. doi: 10.1007/s00210-014-0967-3

6. Roche-Molina, M., Hardwick, B., Sanchez-Ramos, C., Sanz-Rosa, D., Gewert, D., Cruz, F. M., Gonzalez-Guerra, A., Andres, V., Palma, J. A., Ibanez, B., Mckenzie, G., & Bernal, J. A. (2020). The pharmaceutical solvent N-methyl-2-pyrollidone (NMP)

attenuates inflammation through Krüppel-like factor 2 activation to reduce atherogenesis. *Scientific reports*, *10*(1), 11636. doi: 10.1038/s41598-020-68350-2

7. Jeon, O., Bouhadir, K. H., Mansour, J. M., & Alsberg, E. (2009). Photocrosslinked alginate hydrogels with tunable biodegradation rates and mechanical properties. *Biomaterials, 30*(14), 2724-34. doi: 10.1016/j.biomaterials.2009.01.034

Chapter 4: Conclusion and Future Directions

Chemotherapeutics in use today overwhelmingly rely on systemic distribution to deliver drugs to a target cancer site. Systemic distribution results in off-target effects that reduce efficacy, cause toxicity, may lead to irreversible damage, and in many cases decrease patient compliance. Localized delivery of chemotherapy is therefore an ideal method of drug delivery, as local drug delivery systems can decrease systemic effects and allow for higher doses of drug to be used. Hydrogel drug delivery systems are attracting interest in localized drug delivery research due to their high biocompatibility, flexibility, modifiable mechanical properties, tunable degradation rates, and adjustable porosity. Specifically, alginate hydrogel systems show promise due to its low toxicity, chemical versatility, low immunogenicity, and biological inertness. Alginate hydrogel systems have been used in research to facilitate localized delivery of chemotherapeutics and have been used in combination with click chemistry to further increase their stability and create novel drug depot systems that can be noninvasively refilled through the blood.

In this dissertation, an alginate-based drug delivery system for the sustained release of an erlotinib-sulfone-linker conjugate was described. The synthesized erlotinib prodrug demonstrated favorable kinetics with a half-life of 80.454 hours and sustained hydrolytic release of erlotinib from the sulfone-based linker over the course of 30 days. Additionally, erlotinib prodrug showed minimal toxicity against the A431 cell line. Utilization of click chemistry in an alginate-based hydrogel has been previously shown to increase stability and tissue retention, so the strain-promoted azide-alkyne cycloaddition (SPAAC) was used to covalently crosslink alginate strands with the biocompatible click motif, t-BCN. Incorporating this prodrug into a click chemistry-based alginate hydrogel presented some difficulties and needs to be optimized.

Primarily, the ratio of t-BCN molecules to available azide molecules may not be ideal, as crosslinking the low-azide alginate strands required the addition of a calcium sulfate crosslinker. Prodrug was detectable by HPLC in the release buffer, which could support the assertion that the number of t-BCN molecules is not sufficient to crosslink the alginate strands fully and also bind the azides located on the prodrug. Once the ratio of t-BCN to azides is adjusted successfully, a stable crosslinked gel that releases erlotinib in a sustained fashion could be achieved. This gel would need to be tested on a susceptible cell line, such as A431, to ensure both a lack of direct toxicity and establish efficacy of the released erlotinib. T-BCN-linked alginate hydrogels have been tested *in vitro* and *in vivo*, showing that these types of gels are effective and safe in these applications. As such, efficacy of the prodrug-containing hydrogels *in vitro* could lead to *in vivo* testing and eventual success in developing a sustained-release, biocompatible, efficacious drug depot for treating cancers overexpressing EGFR.

In conclusion, the research presented in this dissertation demonstrates several successes. First, the sulfone-based linker developed has minimal toxicity, is tunable, and offers sustained release over the course of 30 days. Second, t-BCN demonstrated potential as a simultaneous crosslinking agent for alginate hydrogels and as an anchor for drug-linker conjugates. Finally, these gels showed at least some stability and release of erlotinib after five days, though there is room to optimize this system. Overall, the t-BCN-linked alginate hydrogel system presented in this dissertation shows promise in the delivery of chemotherapeutics and may offer localized, sustained drug delivery with minimal off-target effects in the future.